Clays and Clay Minerals, Vol. 61, No. 5, 440–460, 2013.

TRACKING FLUID MOVEMENT DURING CYCLIC STEAM STIMULATION OF CLEARWATER FORMATION OIL SANDS USING STABLE ISOTOPE VARIATIONS OF CLAY MINERALS

JENNIFER L. MCKAY[1,*] AND FREDERICK J. LONGSTAFFE[2]

[1]College of Earth, Ocean, and Atmospheric Sciences, Oregon State University, Corvallis, Oregon 97331, USA
[2]Department of Earth Sciences, The University of Western Ontario, London, Ontario N6A 5B7, Canada

Abstract—*In situ* thermal recovery methods such as cyclic steam stimulation (CSS) are required to extract highly viscous bitumen from the Clearwater Formation oil sands of Alberta, Canada. The injection of hot fluids during CSS has altered the mineralogy of the sands, resulting in the loss of some minerals (*e.g.* disseminated siderite, volcanic glass) and precipitation of others (*e.g.* zeolites and abundant hydroxy-interlayered smectite). The high temperatures and high water–rock ratios associated with CSS might also alter the oxygen and hydrogen isotopic compositions of pre-existing clay minerals even in the absence of mineralogical changes. The present study exploits this fact to track the movement of injected hot fluids during CSS. Berthierine, a common diagenetic clay mineral in the Clearwater sands, survived CSS but acquired substantially lower $\delta^{18}O$ and $\delta^{2}H$ values in cores located $\leqslant$10 m from the injection well. In contrast, the oxygen and hydrogen isotopic compositions of berthierine in cores located further from the injection well were generally unaffected, except at the depth of steam injection where horizontal fractures facilitate greater lateral penetration of hot fluids. Smectitic clays in near-injector cores also acquired lower $\delta^{18}O$ values during CSS, but a systematic shift in $\delta^{2}H$ values was not observed. While hydrogen-isotope exchange undoubtedly occurred, the particular combination of temperature and H isotopic composition of the injected fluid used during CSS appears to have yielded post-steam $\delta^{2}H$ values that are indistinguishable from pre-steam values. Only samples from near-injector core G-OB3 that contain hydroxy-interlayered smectite have lower $\delta^{2}H$ values as a result of CSS.

Key Words—Berthierine, Hydrogen Isotopes, Oil Sands, Oxygen Isotopes, Smectite.

INTRODUCTION

The oxygen and hydrogen isotopic compositions of clay minerals are determined in large part by the corresponding isotopic compositions of the water from which they form and the temperature of crystallization, with higher temperature equating to lower $\delta^{18}O$ and higher $\delta^{2}H$ values for a given water composition (Savin and Hsieh, 1998). Other factors also affect the isotopic compositions of clay minerals, including: (1) chemical composition of the clay (Suzuoki and Epstein, 1976; O'Neil, 1987; Savin and Lee, 1988); (2) salinity of the fluid (Horita *et al.*, 1995); and (3) pressure (Horita *et al.*, 1999; Horita *et al.*, 2002). To complicate matters further, the $\delta^{18}O$ and $\delta^{2}H$ values of clay minerals can be modified by exchange after crystallization. Oxygen-isotope exchange is generally negligible below 100ºC (O'Neil and Kharaka, 1976; Yeh and Savin, 1977) but the likelihood of exchange increases at higher temperatures, with significant O-isotope exchange occurring by 300ºC (O'Neil and Kharaka, 1976). Hydrogen is more susceptible to isotopic exchange than oxygen, with measurable H-isotope exchange occurring at 100ºC (O'Neil and Kharaka, 1976) or even lower temperatures given sufficient time and/or high water–rock ratios (Bird and Chivas, 1988; Longstaffe and Ayalon, 1990; Kyser and Kerrich, 1991; Mizota and Longstaffe, 1996).

Oxygen isotopic analysis of clay minerals was shown by Longstaffe (1994) to be useful in defining the extent of steam penetration in the near-wellbore region of the kaolinite-rich Wabiskaw Member oil sands deposit which underlies the Clearwater Formation in the Primrose area of Alberta, Canada (northern portion of the Cold Lake deposit; Figure 1). Clay minerals are ideal for this purpose given their susceptibility to O- and H-isotope exchange at high water–rock ratios and elevated temperatures. In the present study this characteristic of clay minerals was exploited to track the penetration of hot fluids injected into the Clearwater Formation oil sands deposit of Cold Lake, Alberta (Figure 1).

The Lower Cretaceous Clearwater Formation is composed of poorly consolidated sands deposited in a brackish to marine, tide-dominated deltaic environment (Harrison *et al.*, 1981; Visser *et al.*, 1985; McCrimmon and Arnott, 2002). In the Cold Lake area (Figure 1), these sands contain ~29×10^{9} m^{3} of heavy oil and bitumen (ECRB, 2012). Because of the bitumen's high viscosity and relatively deep burial (450–500 m), *in situ* thermal recovery methods such as cyclic steam stimulation (CSS) and steam-assisted gravity drainage (SAGD)

* E-mail addresses of authors:
mckay_jen@yahoo.ca; flongsta@uwo.ca
DOI: 10.1346/CCMN.2013.0610504

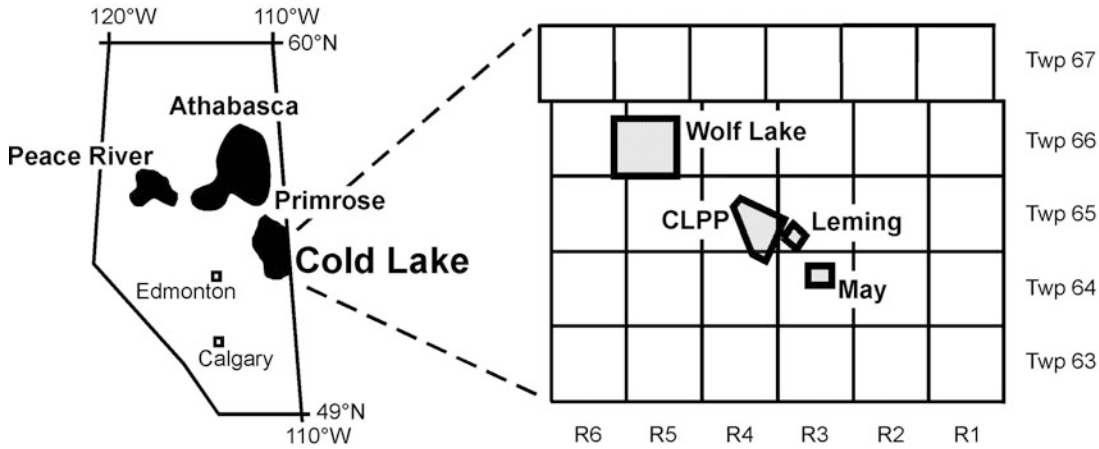

Figure 1. Map showing the Peace River, Athabasca, and Cold Lake oil sands deposits in Alberta, Canada, and the locations of the Wolf Lake, Cold Lake Production Project (CLPP), Leming, and May pilots within the Cold Lake deposits (R – range, Twp – township). The Primrose area of the Cold Lake deposits is located to the north of the study area.

are required for its extraction (Jiang *et al.*, 2010). During CSS, ~80% quality steam (*i.e.* steam to water ratio of 80:20) is injected into the reservoir at temperatures of 250–320ºC and pressures high enough to fracture the reservoir (>10 MPa). Fluid injection continues for at least 1 month, after which the fluid is allowed to sit in the reservoir for a period of time before the bitumen-water mixture is produced from the injection well for several months (Shepherd, 1981; Kry, 1992; Gallant *et al.*, 1993). Each injection-soak-production period is referred to as a cycle and each well undergoes multiple cycles resulting in typical cumulative bitumen recoveries of ~20%. It is believed that the steam-affected zone is ellipsoidal in shape with a major axis aligned along the

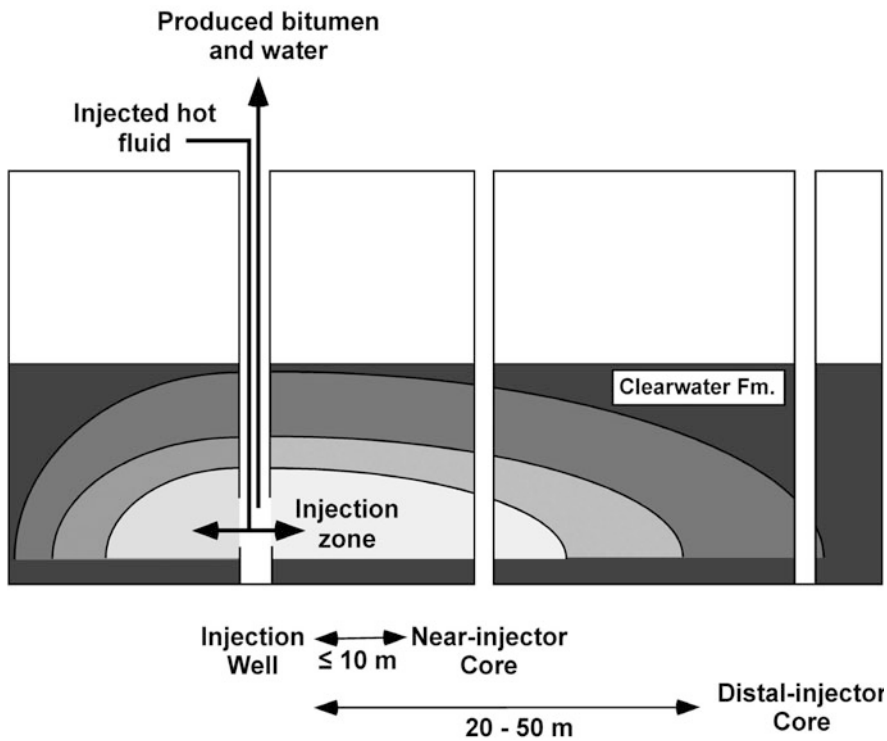

Figure 2. Simplified schematic of the Clearwater Formation oil sands reservoir suggesting how CSS works and the relative locations of near- and distal-injector cores. Injected fluid is thought to move upward and outward (Gallant *et al.*, 1993) resulting in greater bitumen recovery within and above the injection zone (*i.e.* the lightly shaded region) and lower recovery below and further away from the injection zone (*i.e.* the progressively darker shaded regions).

https://doi.org/10.1346/CCMN.2013.0610504 Published online by Cambridge University Press

preferential flow path and that, with each successive cycle, the region of steam contact grows upward and outward from the injection zone (Gallant *et al.*, 1993; Figure 2). Within 10 m of the injection well, the temperature commonly exceeds 100ºC while at 20−50 m from the injection well the temperature is rarely >50ºC (Vittoratos, 1986). Thus, the effects of CSS on bitumen mobilization, mineralogical reactions, and isotopic exchange between clay minerals and the injection fluid and/or bitumen are expected to be greatest near the injection well, at and above the level of steam injection (Longstaffe, 1994). To test this idea, the oxygen and hydrogen isotopic compositions of berthierine and smectitic clays, which are the most abundant clay minerals in both pre- and post-steam Clearwater oil sands, were determined for near-injector ($\leqslant$10 m) and distal-injector (20−50 m) samples.

Five pre-steam cores and eight post-steam cores (four near-injector and four distal-injector) were sampled (Table 1). These cores come from four sites within the Cold Lake oil sands deposit (Wolf Lake, then operated by Amoco, and Leming, May, and the Cold Lake Production Project (CLPP), which were operated by Esso/Imperial Oil; Figure 1). Most post-steam cores were obtained from mid-life CSS operations after 5−9 steam cycles. However, core May B-12A was taken after 18 cycles of steaming by a combination of CSS (steam injection and production from the same vertical well) and steam flooding (steam injection into one vertical well and production from an adjacent vertical well). Fluid was injected into the formation either through a single injection zone (cores BB-13A, OB1, OB4) or through multiple injection zones (May B-12A and all G-OB cores). The injection history for core D23-6A is more complicated. Fluid was first injected near the base of the reservoir for two cycles and then injected at a second zone higher in the formation for four further cycles.

ANALYTICAL TECHNIQUES

All samples contained high concentrations of bitumen, which was removed by Soxhlet extraction (Draper *et al.*, 1955) with toluene following the method described by Fagan (2001). The toluene was then evaporated from the solid and bitumen fractions, both were weighed, and the percentage of bitumen established using these measurements. Soxhlet extraction was generally effective in removing most of the bitumen, although in some post-steam samples trace amounts of pyro-bitumen, a sulfur-rich bitumen-alteration product formed during CSS, remained.

The mineralogy of pre- and post-steam sands was characterized by scanning electron microscopy (SEM), electron microprobe analysis (EMPA), and X-ray diffraction (XRD) analysis of bulk samples and the 2−45 μm and <2 μm size fractions separated *via* settling according to Stokes Law. During this procedure 3% sodium hypochlorite was used to flocculate the <2 μm size fraction after its separation; the clear supernatant was then decanted, and the remaining material was washed repeatedly with distilled water. Preparation of oriented samples of the <2 μm size fraction for XRD analysis involved suction-deposition of K- and Ca-saturated samples onto individual ceramic disks. X-ray diffraction patterns were then obtained in the order listed: (1) K-saturation and heating overnight at 107ºC (0% relative humidity); (2) K-saturation and equilibration over saturated $MgNO_3$ (54% relative humidity); (3) K-saturation and heating to 300ºC for 3 h; (4) K-saturation and heating to 550ºC for 2.5 h; (5) Ca-saturation and equilibration over saturated $MgNO_3$ (54% relative humidity); and (6) Ca-saturation and solvation with ethylene glycol.

The relative percentage of each clay mineral was calculated using the Ca-saturated, ethylene-glycol

Table 1. Pre- and post-steam cores studied[1].

Pre-steam cores	Near-injector cores ($\leqslant$10 m)	Distal-injector cores (20−50 m)	Core location[2]	Reservoir characteristics
May B-12 (11.6%)	May B-12A (4.4%)	n.a.	May	Clean sands with minor clasts and shale layers
G06 (11.1%)	G-OB3 (4.0%)	G-OB1 (9.3%) G-OB2 (9.1%)	Leming	Clean sands
D23-08 (10.5%)	n.a.	D23-6A (7.7%)	CLPP	Abundant clasts, shale layers, and carbonate-cemented zones
BB-12 (9.6%)	BB-13A (7.5%)	n.a.	Leming	Clean sands with many bitumen-poor zones
3L (10.2%)	OB1 (6.5)	OB4 (9.8%)	Wolf Lake	Abundant detrital clays

[1] Average bitumen content given in parentheses.
[2] Refer to Figure 1 for core locations.
n.a.: Core not available.

https://doi.org/10.1346/CCMN.2013.0610504 Published online by Cambridge University Press

solvated and the K-saturated, 550ºC diffraction patterns. For each clay mineral the (001) diffraction intensity was measured and adjusted using form factors (*i.e.* 4×1.0 nm peak, 2×0.7 nm peak, and $1\times$ the most intense diffraction of other phases; Biscaye, 1965).

Concentrated samples of berthierine and smectitic clays for isotopic analysis were prepared by slow-speed centrifugation ($245\times g$) of the <2 μm size fraction to obtain the <1 μm size fraction, followed by high-gradient magnetic separation as described by Hornibrook and Longstaffe (1996). The purity of each concentrate was determined by XRD analysis of a randomly oriented sample and relative mineral abundances were estimated from background-corrected and form-factor-adjusted peak areas of characteristic diffractions. Concentrates containing >70% berthierine were deemed sufficiently pure for isotopic analysis. Separating high-purity smectitic clay was challenging, making it necessary to perform isotopic analysis on concentrates containing, in some cases, only 50% smectite. Isotopic results for these concentrates were corrected for berthierine contamination using the percentages of each clay estimated by XRD and by assuming that: (1) the presence of minor contaminants (quartz, feldspar, illite) had no influence on δ^2H values and negligible influence on $\delta^{18}O$ values; (2) berthierine by weight contains twice as much hydrogen and three-quarters as much oxygen as interlayer water-free smectite, and (3) berthierine in pre-steam and distal-injector cores had $\delta^{18}O$ and δ^2H values similar to average pre-steam berthierine (+11.8‰ and −110‰, respectively) and berthierine in near-injector cores had the same isotopic compositions as the closest berthierine concentrate analyzed.

Prior to isotopic analysis, all clay samples were heated to remove adsorbed and interlayer water, which readily exchanges with atmospheric water at room temperature (Savin and Epstein, 1970). Berthierine samples were pre-treated at 150ºC for 2.5 to 3.0 h as described by Hornibrook and Longstaffe (1996).

The choice of a pre-treatment temperature for smectitic clays was more difficult, given that some smectitic clays can retain residual interlayer water up to 300ºC while structural hydrogen can be released at temperatures as low as 200ºC if the clay is poorly crystallized (Marumo *et al.*, 1995; Fagan and Longstaffe, 1996). Also, the chemical pretreatments used to remove bitumen and organic matter (Soxhlet extraction with toluene and bleaching with sodium hypochlorite) may increase the retention of residual interlayer water in smectites. Failure to remove all interlayer water can lead to δ^2H values that are too high (Fagan, 2001). Because retention of residual interlayer water is heavily dependent on the type of smectitic clay and its interlayer cation composition, *in vacuo* stepwise-heating experiments were conducted on the Clearwater Formation smectites to determine the temperature range over which interlayer water is released. Following the procedure of Marumo *et al.* (1995), the quantity and isotopic composition of hydrogen evolved at 21ºC, from 21−100ºC, in incremental steps of 100ºC between 100 and 600ºC, and from 600−1000ºC were measured for post-steam samples containing smectite (May B-12A-8) and hydroxy-interlayered smectite (HIS; May B-12A-9). A pre-treatment temperature of 150ºC was selected for all smectite-rich samples based on the results of these experiments (Figure 3).

Following pre-heating, structural oxygen was extracted from clay minerals using the BrF_5 method of Clayton and Mayeda (1963) and converted quantitatively to CO_2 over red-hot graphite. The international standard NBS-28 and an in-house quartz standard yielded average $\delta^{18}O$ values of +9.6±0.1‰ (n = 2) and +11.6±0.2‰ (n = 8), respectively, which compare well with expected values of +9.6‰ and +11.5‰. Average $\delta^{18}O$ reproducibility of clay samples was better than ±0.2‰ (n = 3). Structural hydrogen was extracted from clay minerals using the uranium method described by Godfrey (1962) and Kyser and O'Neil (1984). The average δ^2H value obtained for an in-house chlorite standard (−48±2‰; n = 5) compares well with the expected value of −47‰. Average δ^2H reproducibility of clay samples was better than ±2‰ (n = 5). Oxygen- and H-isotope results for the silicates were determined with a two-point VSMOW-SLAP calibration and are reported in the standard δ-notation relative to VSMOW.

The isotopic compositions of two boiler-feed water samples (*i.e.* water from which the steam for CSS was generated) from the Leming pilot were measured by water-CO_2 equilibration for oxygen (Roether, 1970) and by zinc reduction of water for hydrogen (Coleman *et al.*, 1982). One of these boiler-feed waters was generated from Cold Lake freshwater and the other was water produced from the injection well during CSS and recycled back as injected water. An in-house water standard analyzed at the same time yielded a $\delta^{18}O$ value of −7.1‰, which compares well with the expected value of −7.2‰. Reproducibility of $\delta^{18}O$ analyses was better than ±0.1‰. The average δ^2H values of the international standard GISP and an in-house water standard analyzed with each batch of clay and water samples were −191±1‰ (n = 5) and −135 ± 2‰ (n = 13), which compare well with expected values of −190‰ and −136‰, respectively. Oxygen- and H-isotope data for water are reported in the standard δ-notation relative to VSMOW.

RESULTS

Pre-steam mineralogy

The Clearwater Formation sands are unconsolidated, fine- to medium-grained litharenites and feldspathic litharenites (Harrison *et al.*, 1981; Putnam and Pedskalny, 1983; Visser *et al.*, 1985; Prentice and Wightman, 1987). Rock fragments (predominantly

https://doi.org/10.1346/CCMN.2013.0610504 Published online by Cambridge University Press

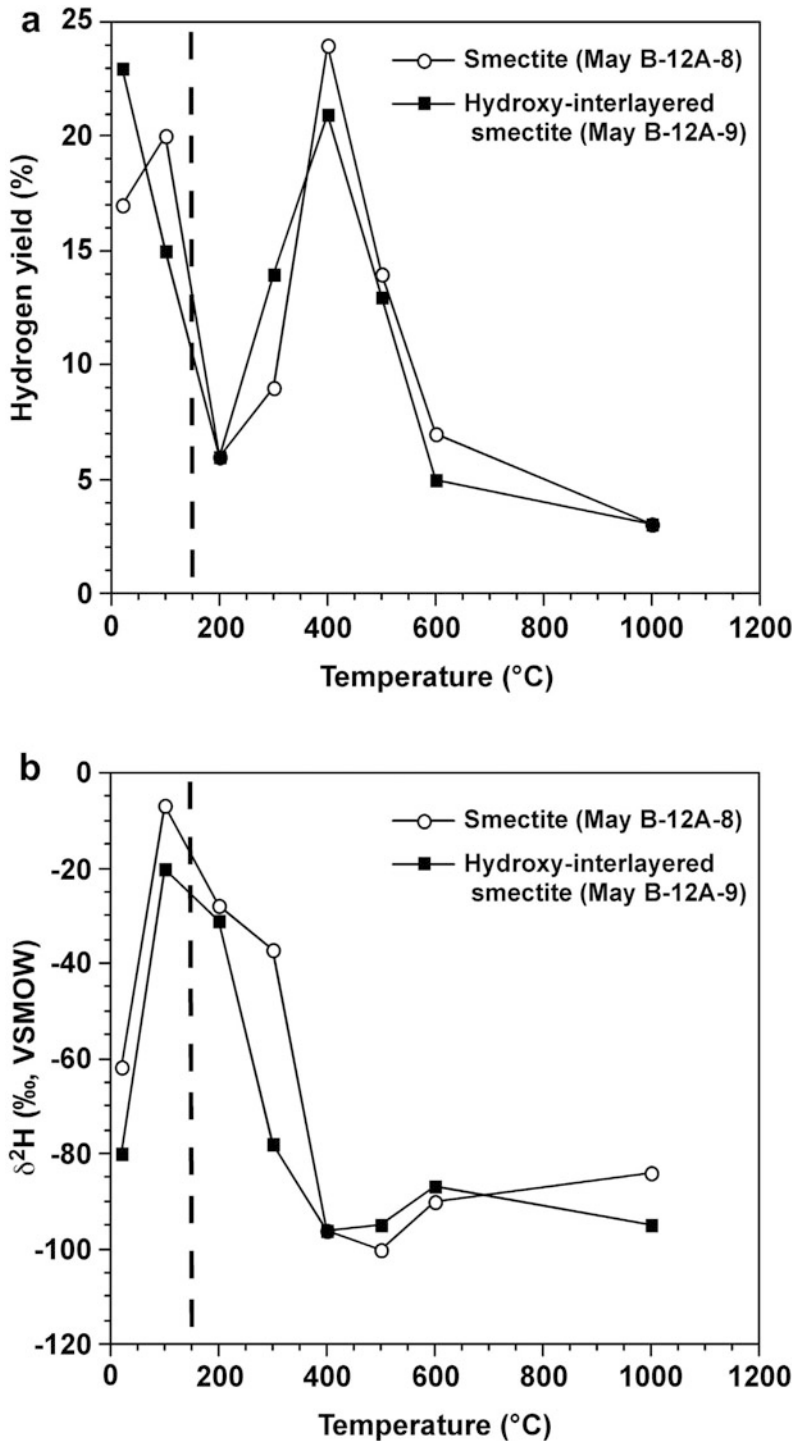

Figure 3. Results of a stepwise-heating experiment to determine: (a) the temperatures at which smectitic clays released adsorbed, interlayer, and structural water *in vacuo*; and (b) the H isotopic composition of that water. Adsorbed water evolved at 21ºC is characterized by low δ^2H values (−62 and −80‰; smectite and HIS, respectively). The majority of interlayer water was evolved between 21 and 100ºC and is characterized by much higher δ^2H values (−20 to −7‰), as was observed by Marumo *et al.* (1995). Residual interlayer water and possibly a very small fraction of the structural hydrogen were released between 100 and 200ºC. However, most of the structural hydrogen, including hydrogen from hydroxy-interlayer material, was released between 200 and 400ºC. Sample May B-12A-9, which contains hydroxy-interlayer material, yields hydrogen at a lower temperature (*i.e.* 300 *vs.* 400ºC) and exhibits a much larger decrease in δ^2H between 200 and 300ºC. Only a minor amount of structural hydrogen was evolved at these temperatures for smectite sample May B-12A-8.

https://doi.org/10.1346/CCMN.2013.0610504 Published online by Cambridge University Press

volcanic grains and chert) are abundant, with lesser amounts of quartz, feldspar, and highly altered grains, and only trace amounts of detrital dolomite. Illite-smectite and illite are the dominant detrital clay minerals (Racki, 1991; Wickert, 1992; McKay and Longstaffe, 1997). These disseminated clays are most abundant in the lower part of the reservoir, as are shale laminae composed of dioctahedral smectite and illite-smectite. Shale clasts containing trioctahedral smectite and siderite are present throughout the formation.

Berthierine is the most abundant diagenetic clay mineral (typically 40–60% of the <2 μm size fraction) and O-isotope data suggest crystallization from a brackish to fresh porewater (Hornibrook and Longstaffe, 1996). Diagenetic smectite and chlorite-smectite are generally restricted to discrete intervals throughout the formation where they typically make up 10–40% of the <2 μm size fraction. As yet, no reliable model exists for predicting where smectitic clays will occur, although O-isotope data suggest that these clays formed in a more marine environment characterized by porewater $\delta^{18}O$ values closer to 0‰ (McKay and Longstaffe, 1997). Kaolinite is limited in abundance and generally restricted to sands near the base of the Clearwater Formation in the Cold Lake area (Abercrombie *et al.*, 1989; Longstaffe *et al.*, 1992). Kaolinite is much more common in the Clearwater Formation reservoir sands of the Primrose area to the north (Beckie and McIntosh, 1989; Longstaffe *et al.*, 1992; Longstaffe, 1994; McKay and Longstaffe, 1997).

A variety of diagenetic minerals is present in the Clearwater Formation at Cold Lake. At least three generations of calcite cements (early grain-coating calcite, Fe-rich pore-filling calcite, and late pore-lining calcite) are present in carbonate-cemented zones that typify the Clearwater Formation (McKay and Longstaffe, 1997). Disseminated, pore-filling siderite (up to 11%) and rare siderite nodules are also present, as are minor to trace quantities of chlorite, clinoptilolite, pyrite, feldspar overgrowths, analcime, halite, and fluorite.

Post-steam mineralogy

The mineralogy of post-steam Clearwater Formation oil sands is similar to that of pre-steam sands with some notable exceptions that are generally restricted to near-injector cores (Table 2). Grain-coating berthierine (Figure 4) remains the most abundant clay mineral (up to 93% of the <2 μm size fraction), even in sands that underwent extensive CSS (*e.g.* core May B-12A). Pre- and post-steam berthierine have a similar lath-like habit and grain-coating texture, and evidence that berthierine was affected during CSS is limited (*e.g.* Figure 4c *vs.* 4d). Pore-filling kaolinite is present in the lowermost reservoir sands in post-steam cores May B-12A, G-OB1, G-OB2, and G-OB3, as it was in the pre-steam sands (Longstaffe *et al.*, 1990; Racki, 1991; this study). A

Table 2. Mineralogical comparison of pre- and post-steam Clearwater sands.

Mineralogy	Pre-steam cores	Post-steam cores	
		Near-injector	Distal-injector
Berthierine	Abundant (40–60% of <2 μm)	No change	No change
Smectitic clays	Present (10–40% of <2 μm)	More abundant and predominantly HIS[1]	Similar abundance, but HIS[1] is present
Kaolinite	Limited, restricted to lower reservoir	No change	No change
Pore-lining chlorite	Not present	Present	Not present
Siderite	Present throughout reservoir	Only found below the uppermost injection zone	No change
Pore-lining calcite	Not present	Present within or near the uppermost injection zone	No change
Carbonate-cemented zones	Present throughout	Minor dissolution at edges	No change
Zeolite	Clinoptilolite (common) Analcime (rare) Wairakite (none)	No change Much more abundant Common	No change No change No change
Rock fragments	Common	Highly dissolved/altered	No change

[1] Hydroxy-interlayered smectite (HIS)

https://doi.org/10.1346/CCMN.2013.0610504 Published online by Cambridge University Press

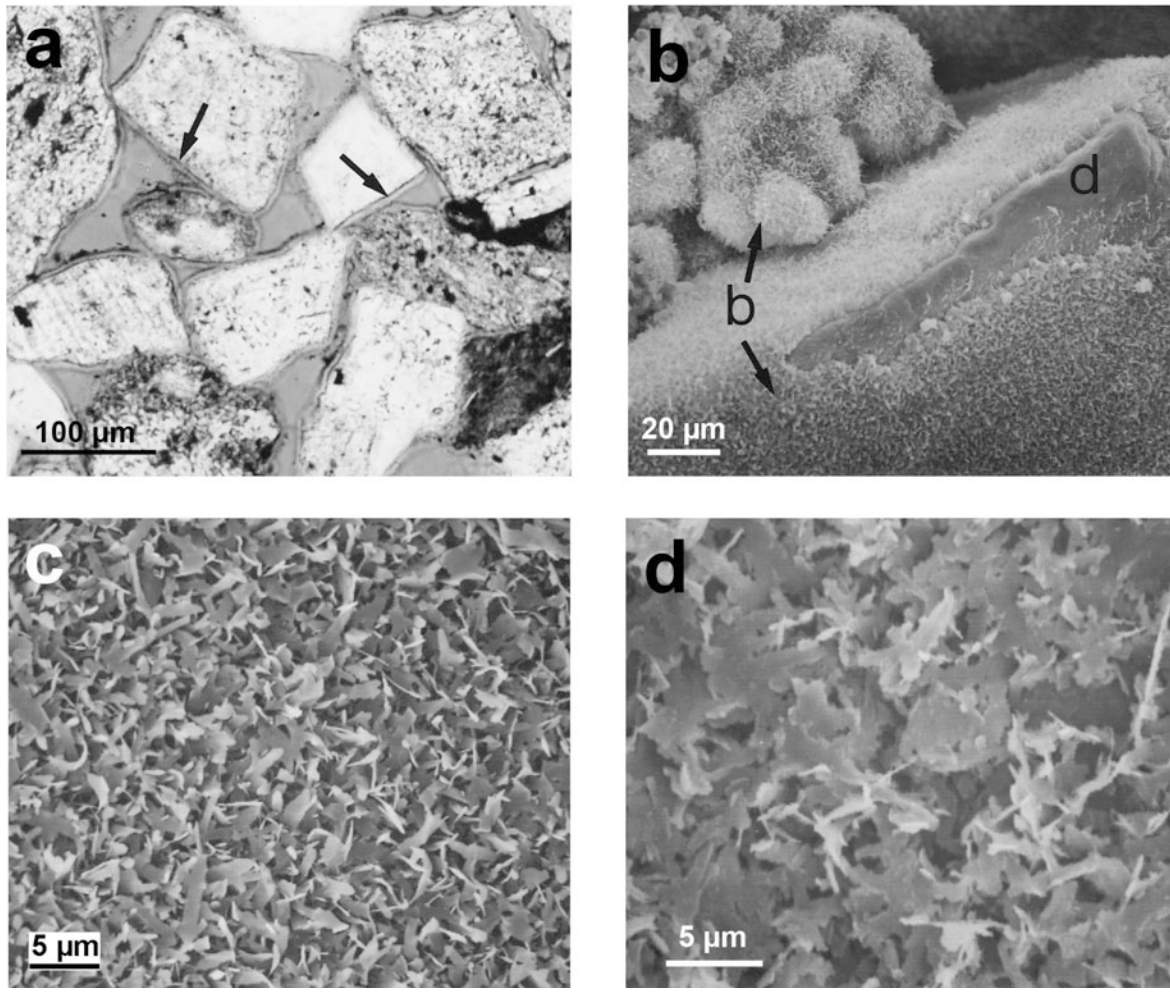

Figure 4. Berthierine in post-steam cores. (a) Photomicrograph (plane-polarized) of grain-coating berthierine (arrows) in near-injector core May B-12A; (b) scanning electron microscope (SEM) image of berthierine (b arrows) coating detrital grains (marked 'd') in distal-injector core GOB2; (c) SEM image of berthierine in distal-injector post-steam core GOB2; the lath-like habit is typical of pre-steam berthierine; (d) SEM image of berthierine in near-injector core May B-12A. Compared to Figure 4c, this berthierine is slightly ragged, possibly reflecting the presence of neoformed smectite, but the typical lath-like habit of berthierine is still recognizable.

variety of smectitic clays, including smectite, chlorite-smectite, illite-smectite, and HIS, were identified in post-steam cores (Figure 5). With the exception of HIS, these smectitic clays are also present in pre-steam cores. Abundant HIS (up to 62% of the <2 µm size fraction) is restricted to post-steam cores, notably near-injector cores May B-12A and G-OB3 (Figure 6). HIS is much less common in distal-injector cores and is not present in pre-steam cores except for BB-12 (Figure 6). The HIS is distinguished in XRD analysis from 'normal' smectitic clays by its failure to collapse to 1.0 nm when heated to 107ºC overnight after K saturation; by comparison, the other smectitic clays undergo almost complete collapse to 1.0 nm under these conditions (Figure 7). Despite its high abundance, however, HIS was impossible to identify petrographically because pre- and post-steam smectitic clays are texturally similar (Figure 5a,b). The only clay neoformed during CSS was an Fe-rich phase (possibly chlorite), which occurs as thick pore-linings associated with volcanic rock fragments (Figure 5c,d). This Fe-rich clay's limited distribution in near-injector cores suggests that it is not HIS.

Diagenetic siderite and sideritized clasts, which occur in minor quantities in pre-steam cores, are absent from most samples from near-injector post-steam cores. The one exception is core G-OB3, which contains siderite in the lowermost portion of the reservoir, 10 m below the uppermost injection zone. Siderite is present in all distal-injector post-steam cores. Cemented zones composed of pore-filling and pore-lining diagenetic calcite (*i.e.* carbonate-cemented zones; Figure 8a,b) are common in all near- and distal-injector cores, suggesting that

https://doi.org/10.1346/CCMN.2013.0610504 Published online by Cambridge University Press

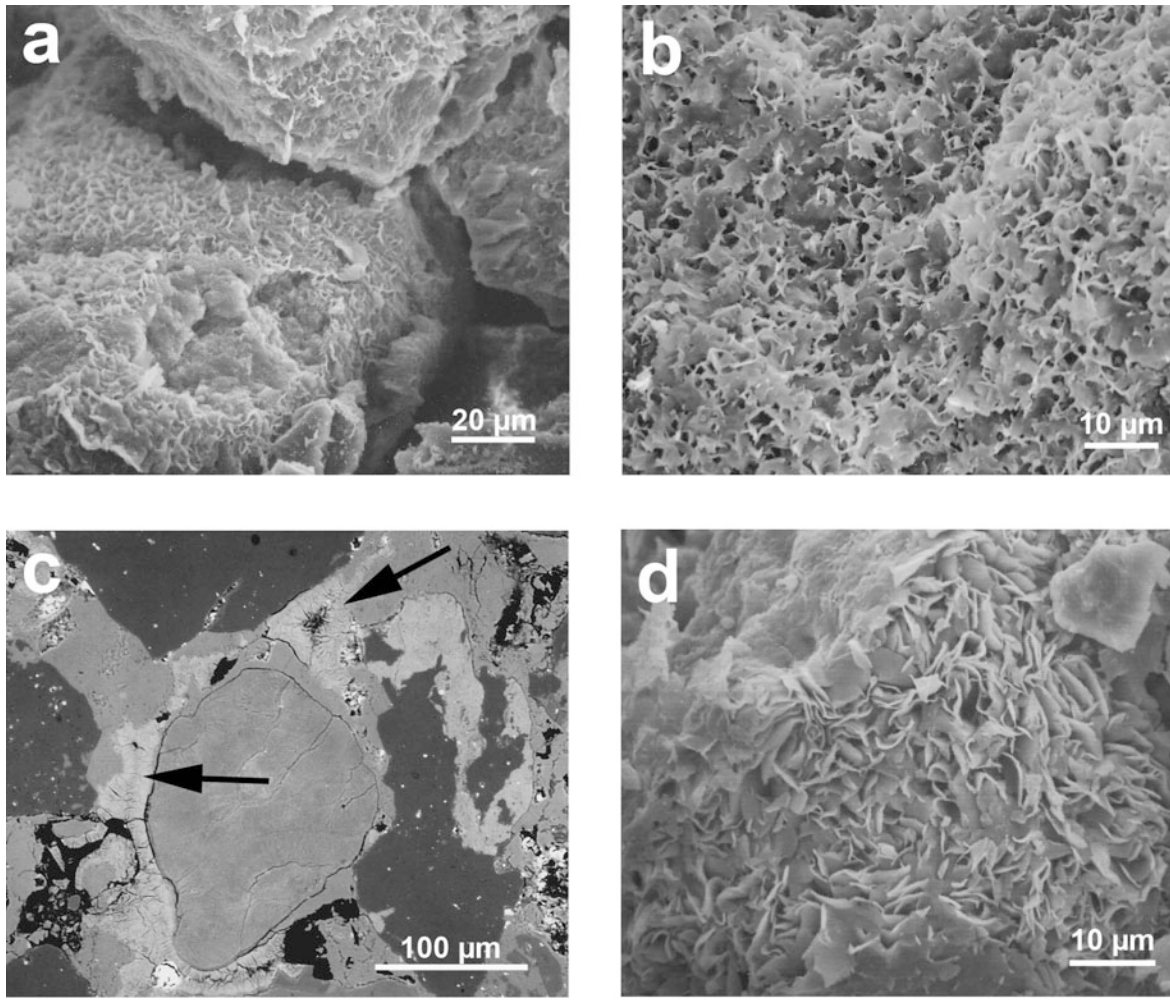

Figure 5. Smectitic clay minerals in post-steam cores. (a–b) SEM images of diagenetic smectitic clay in post-steam core May B-12A; (c) Backscattered electron (BSE) image of pore-lining, Fe-rich clay, possibly chlorite (arrow), which is present exclusively in post-steam cores (sample May B-12A-11); (d) SEM image of Fe-rich clay formed during CSS (sample GOB3-11).

wholesale calcite dissolution did not occur. However, minor calcite dissolution was observed at the edges of some carbonate-cemented zones (Figure 8c). In addition, calcite was precipitated near the injection zone in those post-steam cores where dissolution of carbonate-cemented zones was observed (May B-12A and D23-6A). The meniscus-like, pore-filling habit of this calcite (Figure 8d) suggests growth in a pore system containing immiscible fluids, probably water and hydrocarbons. The composition of this post-steam calcite is highly variable, from pure calcite (99.9 mole% CaO) to Fe- and Mn-rich calcite ($\leqslant$13 mole% FeO and $\leqslant$8.0 mole% MnO).

Three types of zeolite (clinoptilolite, analcime, and wairakite) were identified in the post-steam cores. Clinoptilolite, which occurs as small blocky crystals, is common in pre-steam sands and was apparently unaffected by CSS (Figure 9a,b). Trace amounts of pore-filling analcime occur in pre-steam sands, but it is much more common in post-steam sands (up to 5% of the 2–45 μm size fraction), particularly in smectite-rich zones (Figure 9c,d). Small (10–20 μm) soccer ball-like crystals of wairakite, a Ca-rich zeolite, were observed only in post-steam sands (Figure 9e,f).

Isotopic compositions of pre-steam clays

Previously reported $\delta^{18}O$ values for pre-steam berthierine range from +6.6 to +13.1‰ (Longstaffe *et al.*, 1990, 1992; Hornibrook and Longstaffe, 1996; McKay and Longstaffe, 1997; He, 2001). Corresponding $\delta^{2}H$ values range from −122 to −102‰ (Hornibrook and Longstaffe, 1996; He, 2001). Pre-steam berthierine analyzed during this study has similar oxygen and hydrogen isotopic compositions ($\delta^{18}O$ = +11.0 to +13.4‰; $\delta^{2}H$ = −112 to −106‰; Table 3a).

Pre-steam diagenetic smectitic clay samples mea-

https://doi.org/10.1346/CCMN.2013.0610504 Published online by Cambridge University Press

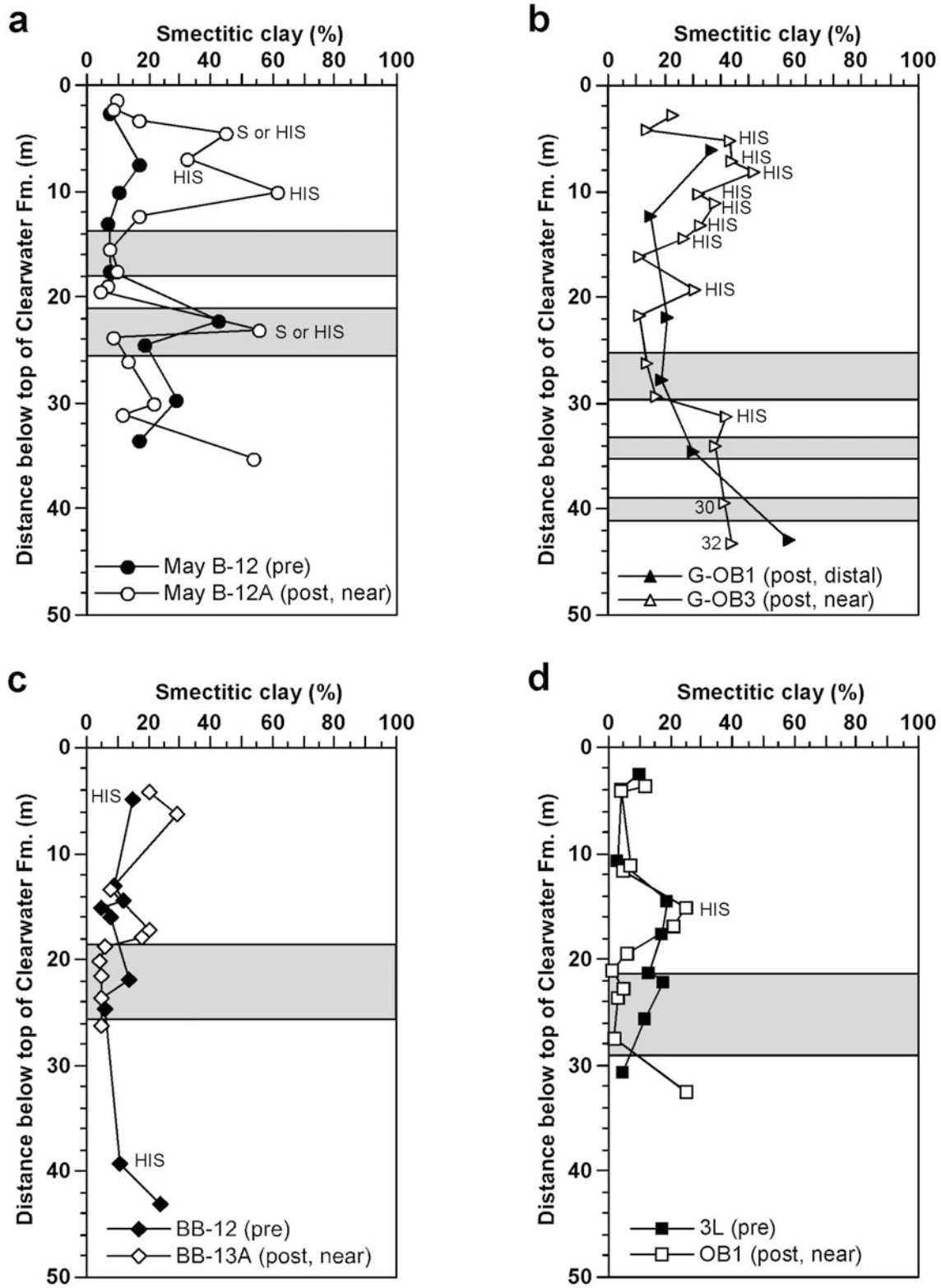

Figure 6. Down-core concentrations of smectitic clay in the <2 μm size fraction of samples from pre- and post-steam cores. The shaded areas indicate injection zones. S = smectite, HIS = hydroxy-interlayered smectite, pre = pre-steam, post = post-steam, near = ⩽10 m from injection well, and distal = 20 to 50 m from injection well.

https://doi.org/10.1346/CCMN.2013.0610504 Published online by Cambridge University Press

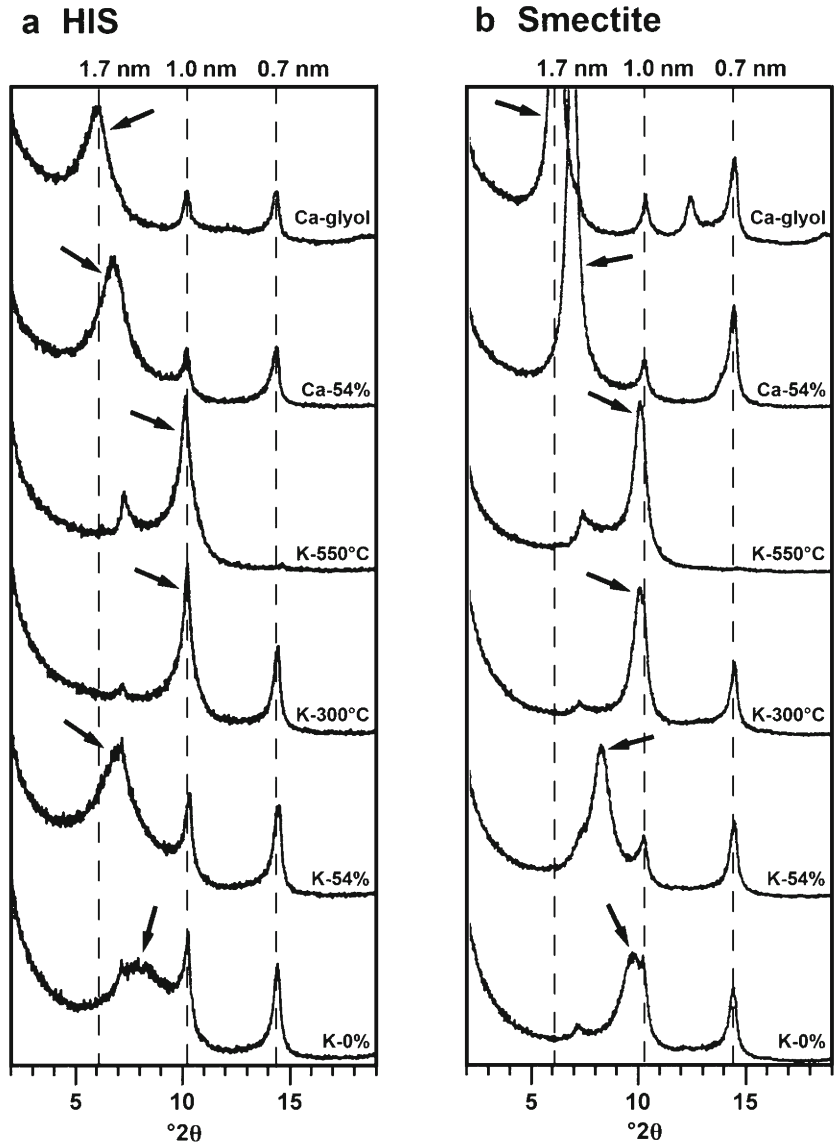

Figure 7. XRD patterns for the <2 μm size fraction for: (a) HIS in sample OB1-16; and (b) smectite in sample May B-12A-28. Arrows indicate the 001 diffraction for HIS or smectite in each diffraction pattern. HIS is differentiated from smectite by a peak between 1.4 and 1.0 nm in the K−0% pattern (this diffraction occurs at ~1.0 nm for 'normal' smectite). Illite (at 1.0 nm) and berthierine ± kaolinite (at 0.7 nm) are also present.

sured in this study have $\delta^{18}O$ values ranging from +18.1 to +20.4‰ following correction for berthierine contamination (Table 4a). These values are similar to those reported by Longstaffe *et al.* (1992) ($\delta^{18}O$ = +18.0 to +18.4‰), but higher than those obtained by He (2001) (+13.9 to +14.7‰). The $\delta^{2}H$ values of pre-steam diagenetic smectite (corrected for berthierine contamination) range from −113 to −98‰ (Table 4a), similar to results obtained by He (2001) (−110 to −106‰). Detrital smectite from a shale clast (pre-steam sample D23-08-17) has a similar O isotopic composition to the diagenetic smectitic clays, but its H isotopic composition is much lower (−123‰, Table 4a).

Isotopic compositions of post-steam clays

Berthierine samples from near-injector, post-steam cores are characterized by lower $\delta^{18}O$ (+0.7 to +6.8‰; average +4.8‰) and $\delta^{2}H$ (−135 to −119‰; average −122‰) values relative to pre-steam berthierine (Figure 10a; Table 3b). The only exception is berthierine from sample OB1-6 (located 17 m above the injection zone), which is isotopically similar to pre-steam berthierine (Figure 10a). There is no evidence that either the O or H isotopic compositions of berthierine in May B-12A, the most extensively steamed core, were altered more than berthierine in other near-injector cores. In most cases, berthierine from distal-injector,

https://doi.org/10.1346/CCMN.2013.0610504 Published online by Cambridge University Press

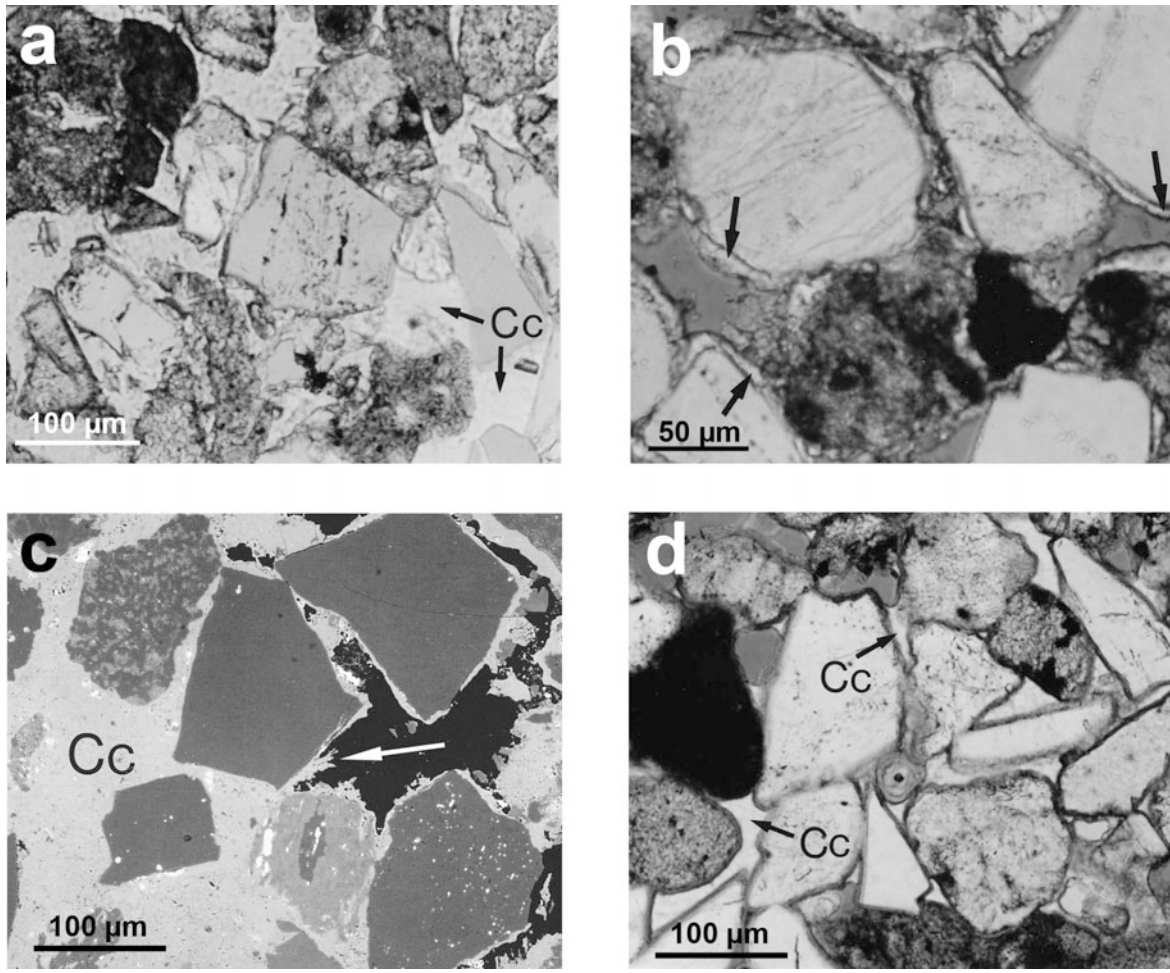

Figure 8. Carbonate cements in post-steam cores. (a) Photomicrograph (crossed polars) of a bitumen-free, carbonate-cemented zone composed of Fe-rich, pore-filling calcite (Cc). These zones are common in both pre- and post-steam cores. (b) Photomicrograph (crossed polars) of a bitumen-saturated, carbonate-cemented zone containing late diagenetic, grain-coating calcite (arrows). Such zones are present in both pre- and post-steam cores. (c) BSE image of a carbonate-cemented zone from post-steam core May B-12A. The carbonate cement (Cc) has ragged edges (arrow) where it contacts the now-vacant pore space (black), which is suggestive of partial dissolution during CSS. (d) Photomicrograph (crossed polars) of calcite (Cc) precipitated during CSS. This calcite typically has a meniscus-like habit (arrows), which is suggestive of growth in a pore system containing immiscible fluids, probably water and hydrocarbon.

post-steam cores is isotopically similar to pre-steam berthierine (Figure 10a; Table 3c). The exception is sample D23-6A-19, which has $\delta^{18}O$ and $\delta^{2}H$ values which are more like those of near-injector berthierine (Figure 10a). This sample is from <0.5 m above the uppermost injection zone in the corresponding injection well (Table 3c).

Post-steam samples rich in diagenetic smectitic clays (*i.e.* excluding shales) have berthierine-corrected $\delta^{18}O$ values of +7.5 to +19.8‰ and $\delta^{2}H$ values of −107 to −80‰ (Table 4b,c). In general, smectitic clays from near-injector cores have lower $\delta^{18}O$ values than pre-steam smectitic clays (Figure 10b). The only exceptions are samples G-OB3-30 and 32, which are located >10 m below the uppermost depth of steam injection; these samples have $\delta^{18}O$ values similar to pre-steam smectitic clays (Figure 10b). In contrast to $\delta^{18}O$, smectitic clays in near-injector cores do not exhibit a systematic shift in $\delta^{2}H$ values (Figure 10b). On closer inspection, however, the $\delta^{2}H$ values of smectitic clays located above the uppermost depth of steam injection in near-injector core G-OB3 (samples 6, 10, and 15; Figure 10b) are lower than the $\delta^{2}H$ values of smectitic clays located well below the uppermost depth of steam injection (*i.e.* samples 30 and 32; Figure 10b). The $\delta^{18}O$ and $\delta^{2}H$ values of smectitic clays from distal-injector cores are generally similar to pre-steam smectitic clays (Figure 10b).

Detrital smectitic clays from shale layers and clasts in both near- and distal-injector cores exhibited larger differences in terms of $\delta^{18}O$ with respect to pre-steam clay (>11‰ lower than the pre-steam shale sample) than the diagenetic smectitic clays. No significant difference

https://doi.org/10.1346/CCMN.2013.0610504 Published online by Cambridge University Press

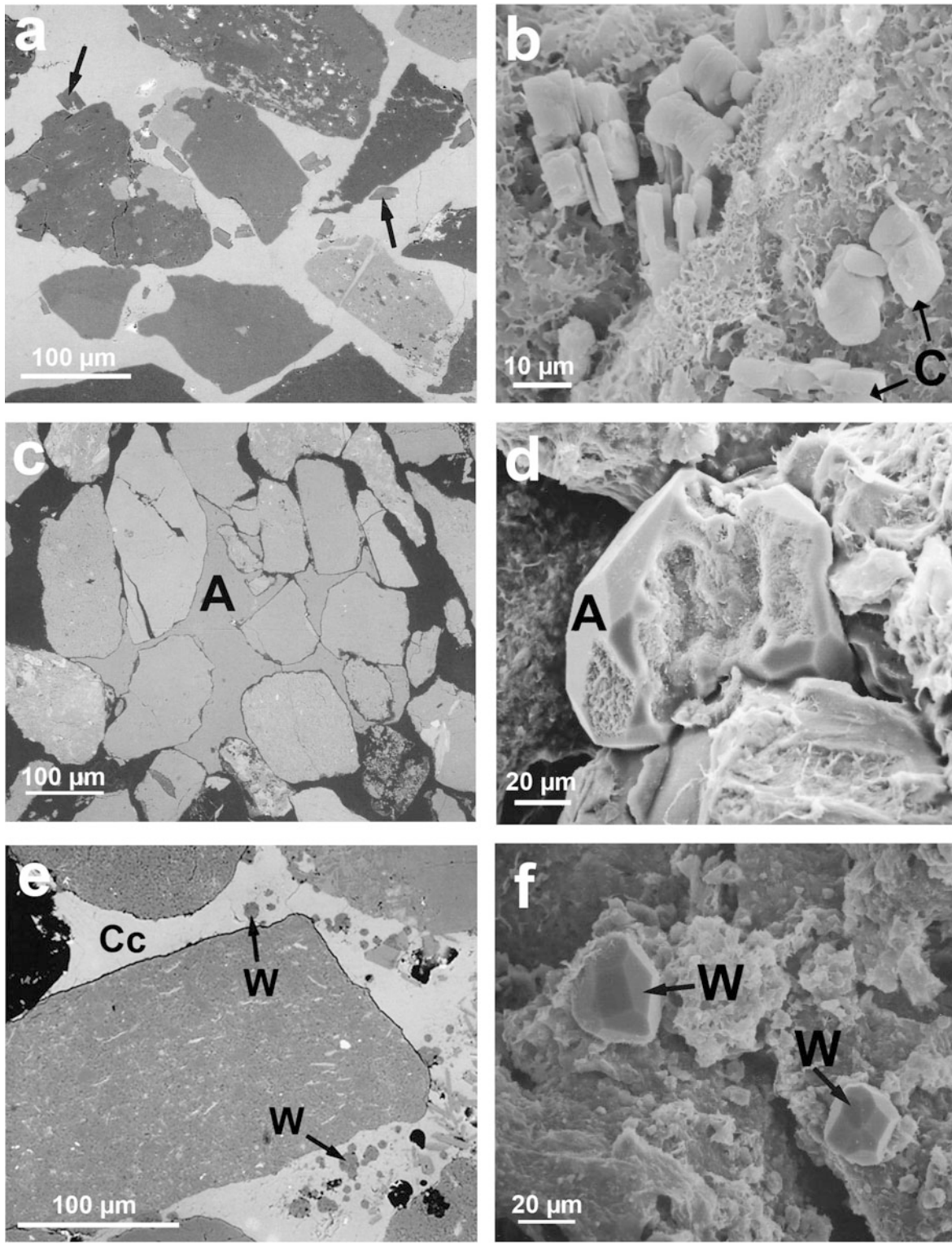

Figure 9. Zeolites in post-steam cores. (a) BSE image of tabular crystals of early diagenetic clinoptilolite (arrows) within a calcite-cemented zone (core May B-12A); (b) SEM image of clinoptilolite (C) and smectitic clay (possibly HIS) in post-steam sample May B-12A-9; (c) BSE image of pore-filling analcime (A) in post-steam core May B-12A; (d) SEM image of analcime (A) in post-steam sample GOB3-32; (e) BSE image of small (10–20 µm) crystals of wairakite (W) formed during CSS prior to crystallization of post-steam calcite (Cc); (f) SEM image of wairakite (W) formed during CSS.

https://doi.org/10.1346/CCMN.2013.0610504 Published online by Cambridge University Press

Table 3a. Oxygen- and hydrogen-isotope results for pre-steam berthierine.

Core/Sample	$\delta^{18}O$	$\delta^{2}H$	Mineralogy[1]
	– (‰, VSMOW) –		
D23-08-10	+11.0	−111	81B, 17S, 2Q
BB-12-8	+11.2	−106	84B, 15S, 1Q
3L-4	+11.3	−110	76B, 18S, 2Q, 2I, 2F
3L-7	+12.0	−112	83B, 14S, 3Q
3L-22	+13.4	−110	77B, 20S, 3Q

Table 3b. Oxygen- and hydrogen-isotope results for near-injector berthierine.

Core/Sample	$\delta^{18}O$	$\delta^{2}H$	Mineralogy[1]	Location relative to injection zone(s)[2]
	— (‰, VSMOW) —			
May B-12A-3	+6.3	−119	74B, 19S, 4Q, 3I	12.0 m above upper IZ
May B-12A-21	+4.8	−120	86B, 12S, 2Q	between upper and lower IZs
May B-12A-23	+5.3	−120	82B, 16S, 2Q	between upper and lower IZs
G-OB3-12	+3.6	−119	93B, 6S, 1Q	9.0 m above upper IZ
G-OB3-18	+3.0	−124	90B, 4S, 2Q, 2I, 2F	3.5 m above upper IZ
BB-13A-436.24	+6.8	−123	84B, 16S, <1Q	5.0 m above IZ
BB-13A-9	+4.2	−119	89B, 11S, <1Q	in IZ
BB-13A-12	+3.1	−128	86B, 13S, 1Q	0.5 m below IZ
OB1-6	+10.6	−114	97B, 3S, <1Q	17.0 m above IZ
OB1-28	+0.7	−135	86B, 12S, 2Q	in IZ

Table 3c. Oxygen- and hydrogen-isotope results for distal-injector berthierine.

Core/Sample	$\delta^{18}O$	$\delta^{2}H$	Mineralogy[1]	Location relative to injection zone(s)[2]
	– (‰, VSMOW) –			
G-OB1-5	+10.7	−108	87B, 12S, 1Q	15.5 m above upper IZ
G-OB1-11	+12.1	−113	78B, 21S, 1Q	in upper IZ
G-OB2-3	+12.1	−109	79B, 20S, 1Q	19.0 m above upper IZ
G-OB2-6	+11.5	−104	74B, 25S, 1Q	2.5 m above upper IZ
G-OB2-9	+12.2	−110	76B, 22S, 2Q	in upper IZ
D23-6A-4	+12.1	−109	80B, 19S, 1Q	25.5 m above upper IZ
D23-6A-5	+10.7	−114	89B, 10S, 1Q	23.0 m above upper IZ
D23-6A-7	+11.8	−103	70B, 28S, 2Q	19.0 m above upper IZ
D23-6A-11	+12.8	−111	72B, 20S, 5Q, 3F	10.5 m above upper IZ
D23-6A-14	+11.9	−106	83B, 15S, 2Q	8.0 m above upper IZ
D23-6A-17	+10.5	−105	91B, 8S, 1Q	4.5 m above upper IZ
D23-6A-19	+6.7	−119	90B, 6S, 4Q	<0.5 above upper IZ
D23-6A-26	+9.2	−112	88B, 11S, 1Q	10.0 m below upper IZ, 5 m above lower IZ
OB4-3	+11.3	−102	86B, 13S, 1Q	16.5 m above IZ
OB4-10	+13.0	−106	79B, 20S, 1Q	5 m above IZ

[1] Percentage of berthierine (B), smectitic clay (S), quartz (Q), illite (I), and feldspar (F) estimated from XRD.
[2] IZ – Injection zone

was observed, however, in $\delta^{2}H$ values compared to the range of pre-steam smectite values (Figure 10b).

Isotopic compositions of boiler-feed water

There was no opportunity to sample boiler-feed water, steam condensate, or produced water at the time of CSS. Two boiler-feed water samples were obtained from the Leming pilot shortly thereafter, however. One sample of treated fresh surface water has $\delta^{18}O$ = −11.4‰ and $\delta^{2}H$ = −107‰. The second sample (recycled produced water) has $\delta^{18}O$ = −12.6‰ and $\delta^{2}H$ = −122‰. The similarity in $\delta^{18}O$ values of these two waters suggests that CSS had little effect on the O isotopic composition of the produced water. The lower $\delta^{2}H$ value of the produced water may indicate hydrocarbon contamination, or H-exchange between the water

https://doi.org/10.1346/CCMN.2013.0610504 Published online by Cambridge University Press

Table 4a. Oxygen- and hydrogen-isotope results for pre-steam smectitic clays.

Core/Sample	$\delta^{18}O$ (‰, VSMOW)[1]	$\delta^{2}H$ (‰, VSMOW)[1]	Mineralogy[2]
May B-12-11	+18.5 (+20.4)	−112 (−113)	68S, 25B, 4Q, 3F
G06-9	+16.8 (+18.1)	−103 (−98)	68S or CS, 23B, 6Q, 3I
D23-08-17 (shale clast)	+18.4 (+19.1)	−120 (−123)	83DiS or CS, 11B, 6Q
BB-12-13[1]	+16.0 (+18.3)	−110 (−110)	55S, 40B, 5Q

Table 4b. Oxygen- and hydrogen-isotope results for near-injector smectitic clays.

Core/Sample	$\delta^{18}O$ (‰, VSMOW)[1]	$\delta^{2}H$ (‰, VSMOW)[1]	Mineralogy[2]	Location relative to injection zone(s)[3]
May B-12A-1 (shale)	+0.2 (+0.2)	−121 (−121)	89DiS ± IS, 8Q, 3I	14.0 m above upper IZ
May B-12A-4 (shale clast)	+4.9 (+4.8)	−119 (−119)	88TriS, 8B or K, 4Q	12.0 m above upper IZ
May B-12A-8	+9.9 (+10.7)	−109 (−102)	73S or HIS, 22B, 5Q	9.0 m above upper IZ
May B-12A-9	+13.8 (+16.1)	na	67HIS, 27B, 6Q	6.5 m above upper IZ
May B-12A-12	+13.4 (+14.6)	−105 (−99)	80HIS, 15B, 5Q	3.5 m above upper IZ
May B-12A-28	+6.8 (+7.5)	−109 (−97)	62S or HIS, 35B, 3Q	In lower IZ
May B-12A-38 (shale)	+7.4 (+7.5)	−109 (−108)	89DiS ± IS, 5B, 6Q	7.5 m below lower IZ
May B-12A-41	+7.3 (+8.2)	−106 (−91)	61S, 34B, 5Q	9.5 m below lower IZ
G-OB3-6	+7.8 (+9.0)	−107 (−98)	70HIS, 25B, 4Q, 1I	18.0 m above upper IZ
G-OB3-10	+7.8 (+9.9)	−108 (−94)	56HIS, 35B, 4Q, 1I, 4F	12.0 m above upper IZ
G-OB3-15	+8.3 (+11.7)	−107 (−87)	46HIS, 40B, 6Q, 3I, 5F	6.0 m above upper IZ
G-OB3-23	+9.0 (+11.9)	−107 (−84)	58S or HIS, 39B, 3Q	1.5 m below upper IZ
G-OB3-26	+13.1 (+13.9)	−101 (−85)	50CS, 44B, 3Q, 3F	4.5 m below upper IZ, in middle IZ
G-OB3-30	+15.2 (+17.1)	−100 (−85)	54CS, 40B, 4Q, 2I	9.5 m below upper IZ, in lower IZ
G-OB3-32	+17.1 (+19.8)	−97 (−80)	56CS, 37B, 4Q, 3I	13.5 m below upper IZ, 1.0 m below lower IZ
BB-13A-4	+9.4 (+10.7)	−112 (−98)	53CS, 34B, 10Q, 3I	12.0 m above IZ

Table 4c. Oxygen- and hydrogen-isotope results for distal-injector smectitic clays.

Core/Sample	$\delta^{18}O$ (‰, VSMOW)[1]	$\delta^{2}H$ (‰, VSMOW)[1]	Mineralogy[2]	Location relative to injection zone(s)[3]
G-OB2-10	+16.3 (+17.7)	−108 (−106)	67S or CS, 28B, 3Q, 2I	1.5 m below upper IZ
G-OB2-11	+16.9 (+17.9)	−106 (−103)	77HIS, 20B, 3Q	4.0 m below upper IZ, in middle IZ
G-OB2-12	+18.5 (+19.7)	−108 (−107)	77HIS, 18B, 5Q	6.5 m below upper IZ, 1 m below middle IZ
G-OB2-13	+15.9 (+17.3)	−104 (−100)	62S, 28B, 6Q, 7I	10.0 m below upper IZ, in lower IZ
G-OB2-15	+16.9 (+18.6)	−102 (−95)	66HIS, 29B, 5Q	13.0 m below upper IZ, 1.5 m below lower IZ
G-OB1-18	+15.7 (+17.9)	−98 (−80)	52S, 39B, 7Q, 2I	10.5 m below upper IZ, within lower IZ
D23-6A-513m (shale)	+6.1 (+5.8)	−113 (−114)	90TriS, 6B, 4Q	In lower IZ

[1] Results following correction for berthierine contamination are given in parentheses.
[2] Percentage of smectitic clay (S), dioctahedral smectitic clay (DiS), trioctahedral smectitic clay (TriS), hydroxy-interlayered smectite (HIS), chlorite-smectite (CS), quartz (Q), illite (I), and feldspar (F) estimated by XRD.
[3] IZ = Injection zone

and bitumen (bitumen $\delta^{2}H = -138‰$; Marcano, 2011), or it may simply reflect disproportionate recovery of steam-condensate compared to total injected fluid. Boiler-feed water samples from other pilot sites in the Cold Lake area have similar isotopic compositions ($\delta^{18}O = -12.1$ to $-11.3‰$; $\delta^{2}H = -123$ to $-104‰$; He, 2001).

DISCUSSION

Mineralogical changes

In near-injector cores, CSS has caused complete dissolution of siderite, minor dissolution of carbonate-cemented zones, alteration of the glassy matrix of volcanic rock fragments, and precipitation of calcite, zeolites (analcime and wairakite), and an Fe-rich clay

https://doi.org/10.1346/CCMN.2013.0610504 Published online by Cambridge University Press

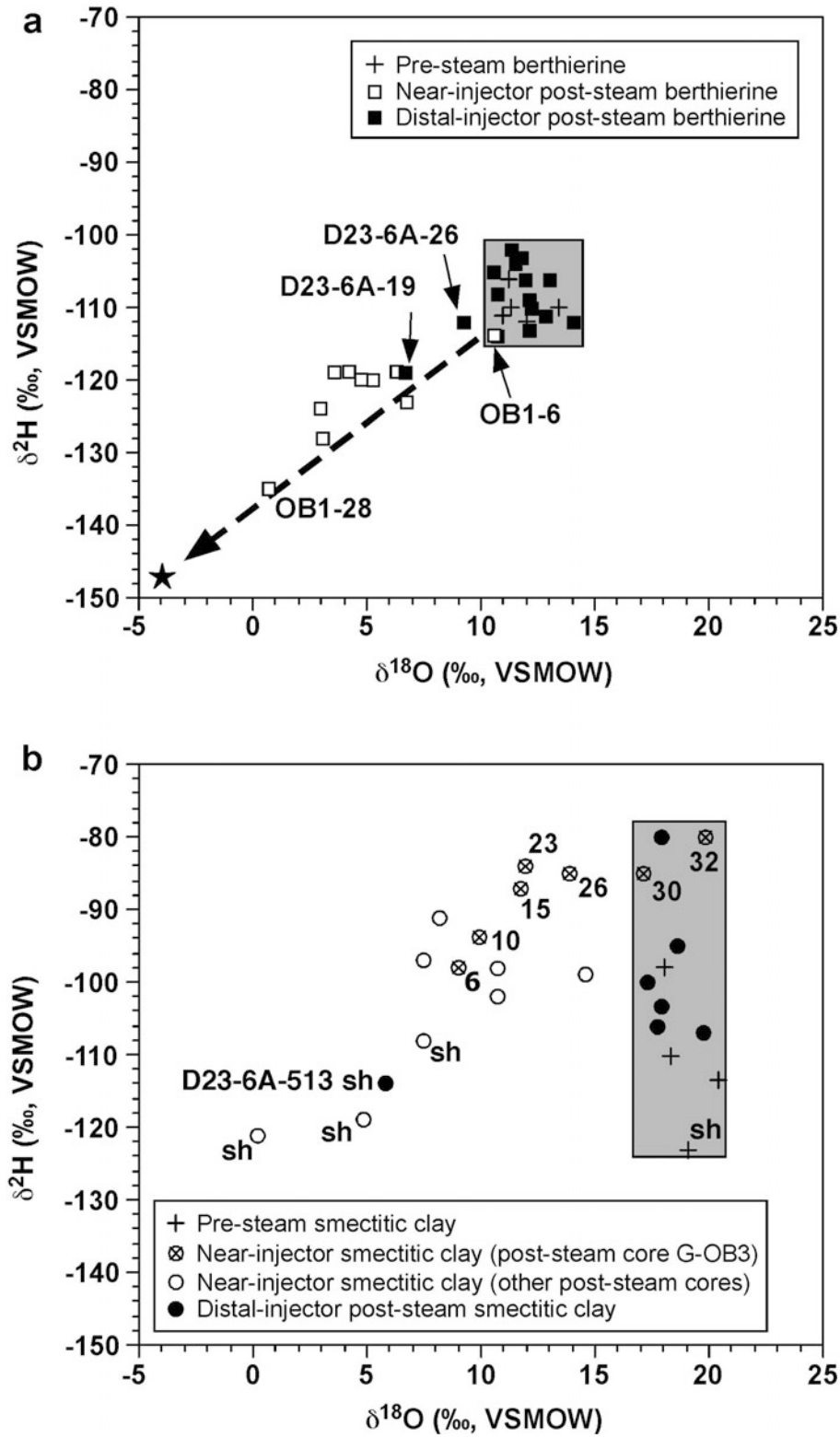

Figure 10. Hydrogen *vs.* oxygen isotopic compositions of (a) pre- and post-steam berthierine and (b) pre- and post-steam smectitic clays, including shale layers and clasts (sh). Near-injector berthierine samples trend toward the predicted $\delta^{18}O$ and $\delta^{2}H$ values for berthierine that has completely exchanged at 150ºC with an injected fluid of $\delta^{18}O = -12‰$ and $\delta^{2}H = -107‰$ (★ in Figure 10a. The shaded boxes outline the ranges in $\delta^{18}O$ and $\delta^{2}H$ values of pre-steam and distal-injector clays analyzed during the present study.

https://doi.org/10.1346/CCMN.2013.0610504 Published online by Cambridge University Press

mineral (possibly chlorite). Similar results were obtained during previous experimental, modeling, and post-steam core studies (Boon, 1977; Perry and Gillott, 1979; Sedimentology Research Group, 1981; Boon and Hitchon, 1983; Boon *et al.*, 1983; Hutcheon, 1984; Hebner *et al.*, 1986; Lefebvre and Hutcheon, 1986; Kirk *et al.*, 1987; Gunter and Bird, 1988; Gunter *et al.*, 1989; Tilley and Gunter, 1988; Cathles *et al.*, 1990; Hutcheon and Abercrombie, 1990; Shevalier *et al.*, 1992; Fialka *et al.*, 1993; Chakrabarty and Longo, 1994; Longstaffe, 1994; Mok *et al.*, 1995; Zhou *et al.*, 1995, 1999; He, 2001). Many of these studies also documented neoformation of smectitic clays in accord with the present results. Above the injection zone in near-injector cores May B-12A and G-OB3, the abundance of smectitic clay is substantially greater than in corresponding pre-steam cores (Figure 6a,b). This zone of smectite enrichment coincides with the occurrence of HIS, which is characteristic of post-steam cores and particularly abundant in some near-injector cores. However, not all near-injector cores are characterized by an increase in smectitic clay content. The amounts of smectitic clays in near-injector cores BB-13A and OB1 are similar to those in pre-steam cores and HIS is limited (Figure 6c,d). Pre-steam texture, particularly the presence of abundant grain-coating bertherine, could have limited the formation of smectitic clay in these cores by isolating reactive rock fragments and detrital carbonate. Solution pH may also have influenced the formation of smectite because it controls the dissolution of carbonate, which supplies cations for smectite formation (Gunter and Bird, 1988; Hutcheon *et al.*, 1990). Carbonate dissolution is also responsible for the production of large quantities of CO_2 during CSS (Hutcheon *et al.*, 1989, 1990; Cathles *et al.*, 1990). Water produced from late cycle wells at the Leming pilot is close to chemical equilibrium with calcite (Abercrombie *et al.*, 1989), thus explaining the precipitation of calcite (Figure 8d) in near-injector cores May B-12A and D23-6A.

Mineralogical changes that were expected, but not observed, are equally important to consider. Berthierine is the most common clay mineral in pre-steam Clearwater Formation oil sands within the Cold Lake area, and also in post-steam sands, even for cores that experienced extensive CSS. For example, the <2 μm size fraction in pre-steam core May B-12 contains an average of 55% berthierine. The corresponding <2 μm size fraction in near-injector post-steam core May B-12A retains an average of 40% berthierine, despite the sands having undergone 18 steam injection/production cycles. The wholesale conversion of berthierine to Fe-saponite observed in laboratory experiments (Zhou *et al.*, 1995, 1999) was not observed in this field study. Moreover, little textural evidence was found that berthierine was modified significantly by CSS, although it was overgrown by neoformed smectitic clay in some samples (Figure 4b). Zhou *et al.* (1995) studied the reactivity of berthierine in acidic, neutral, and alkaline solutions at various temperatures, and found that berthierine altered rapidly to Fe-rich smectite and analcime in alkaline solutions at 250ºC. However, at lower temperatures (150ºC) and lower pH (neutral to acidic conditions), berthierine reactivity was limited (Zhou *et al.*, 1995, 1999), which appears to have been the case for the cores examined in the present study. In turn, the preservation of grain-coating berthierine has served to isolate highly reactive rock fragments (a source of Si and other cations; Dudley and Moore, 1992; Huang and Longo, 1994) from injected fluids, further limiting smectite formation. Such armoring may explain why near-injector cores from berthierine-rich regions (cores BB-13A and OB1) contain little HIS. The low abundance of other reactants (*e.g.* kaolinite and disseminated carbonates) and their distribution in the Clearwater Formation also probably played a role in restricting smectite formation. Abundant kaolinite is present only in the lowermost portion of the reservoir, below the depth of steam injection in most of the post-steam cores studied. The preservation of kaolinite even in near-injector cores indicates that interaction between the injected fluid and reservoir sands was limited below the injection zone, probably because of the steam's tendency to move upward and the reduced permeability in the lower portion of the reservoir arising from abundant detrital clays and shale laminae.

Isotopic changes

Determining the extent of fluid–rock interaction from mineralogical data alone is difficult because the effects are not simply related to the presence or absence of the injected fluid. For example, lack of HIS formation could mean that: (1) a portion of the reservoir was not heated by contact with hot fluids; (2) components necessary to form HIS (*e.g.* rock fragments, disseminated carbonates, and kaolinite) were not present; and/or (3) grain-coating berthierine shielded reactive components from injected fluids. Comparison of the oxygen and hydrogen isotopic compositions of pre- and post-steam clay minerals (berthierine and smectitic clays) provides a means to better understand the effects of CSS on the reservoir.

Berthierine. While berthierine was preserved during CSS, the evidence is clear that isotopic exchange in near-injector cores resulted in lower $\delta^{18}O$ and $\delta^{2}H$ values (Figure 10a). Only one near-injector berthierine sample was unaffected (OB1-6, Figure 10a), probably because of its large distance (17 m) above the injection zone and the presence of a shale barrier between this sample and the underlying injection zone. In contrast to near-injector cores, the O and H isotopic compositions of berthierine in distal-injector cores were unaffected by CSS with the exception of sample D23-6A-19 (Figure 10a). The lack of change suggests that:

https://doi.org/10.1346/CCMN.2013.0610504 Published online by Cambridge University Press

(1) berthierine did not undergo isotopic exchange below ~100ºC (the maximum temperature in distal-injector well G-OB2); or (2) the injected fluid did not penetrate the distal reservoir because bitumen saturation remained too high and hence permeability was too low. That said, distal-injector sample D23-6A-19, from a depth corresponding to the top of the injection zone, did undergo isotopic exchange, suggesting that hot fluids moved horizontally from the injection zone and through the formation for at least 20 m, probably following fractures created during fluid injection. However, fluid movement was restricted vertically, as indicated by the lack of O and H isotope exchange in sample D23-6A-17, located only 4.0 m above sample D23-6A-19 (Table 3).

The temperature and isotopic compositions of the injected fluid must be known to calculate the extent of O-isotope exchange affecting these clay minerals. Boiler-feed water from the Leming pilot had $\delta^{18}O$ values of −12.6 and −11.4 ‰ (average −12‰), similar to boiler-feed water and steam condensate from other Cold Lake pilot sites (He, 2001). Vittoratos (1986) suggested that the temperatures in near-injector cores commonly exceeded 100ºC. Using the berthierine-water O-isotope geothermometer of Hornibrook and Longstaffe (1996) [$1000\ln\alpha_{berthierine\text{-}H_2O} = 5.174(10^3)T^{-1} + 2.483(10^6)T^{-2} - 0.430(10^9)T^{-3} + 0.039(10^{12})T^{-4} - 13.59$], and assuming complete re-equilibration at $\geqslant$100ºC with the boiler feed water ($\delta^{18}O$ = −12‰), yields berthierine with $\delta^{18}O$ values of <0‰ (*e.g.* −4‰ at 150ºC). In reality, only one near-injector berthierine sample (OB1-28, $\delta^{18}O$ = +0.7‰; Figure 10a) has a $\delta^{18}O$ value close to the predicted value. Most near-injector berthierine $\delta^{18}O$ values are higher (+3.1 to +6.8‰) indicating either: (1) complete isotopic exchange at relatively low temperatures (40−90ºC); or (2) incomplete isotopic exchange at higher temperatures (*e.g.* 30−70% at 150ºC). Option 1 is unlikely given that the O isotopic composition of berthierine in distal-injector cores was generally unaffected at such temperatures. Option 2 is supported by the fact that near-injector berthierine samples trend toward the predicted $\delta^{18}O$ value for complete isotopic exchange at 150ºC from a water of −12‰ (Figure 10a). The apparent absence of O-isotope exchange between berthierine and injected fluids in the distal-injector cores may indicate that reservoir temperatures were not high enough for long enough to cause exchange. The injected fluids were less likely, however, to penetrate this portion of the reservoir because of the presence of bitumen in the pore space. Distal-injector cores contain 7.7 to 9.8% bitumen (~80% of original bitumen content) whereas near-injector cores contain 4.0 to 7.5% bitumen (~50% of original bitumen content) (Table 1).

Hydrogen-isotope exchange between clay minerals and water typically occurs more readily and at lower temperatures than O-isotope exchange (O'Neil and Kharaka, 1976; Bird and Chivas, 1988; Longstaffe and Ayalon, 1990; Sheppard and Gilg, 1996). Thus, H-isotope exchange was expected for berthierine from both near-injector and distal-injector cores. However, with the exception of sample D23-6A-19, evidence for H-isotope exchange is restricted to near-injector cores (Figure 10a). The lack of H-isotope exchange in distal-injector cores is probably due to the combination of low reservoir temperatures during CSS and limited bitumen mobilization, which restricted penetration of injected fluids. For near-injector samples, the extent of H-isotope exchange can be estimated using an injected fluid δ^2H of −107‰, the value for boiler-feed water derived from fresh surface water, and by assuming that the chlorite-water H-isotope fractionation factor of −40‰ (Marumo *et al.*, 1980) is applicable to berthierine at CSS temperatures. In reality, the H-isotope fractionation is probably >40‰ because berthierine has a higher Fe/(Fe+Mg) ratio (Marumo *et al.*, 1980; Sheppard and Gilg, 1996); how much larger, however, is unknown. Under these conditions, completely exchanged berthierine should have a δ^2H value of −147‰ or lower. Instead, measured δ^2H values are higher (−135 to −119‰) suggesting incomplete H-isotope exchange. Given that the data plot close to the theoretical trend line for O- and H-isotope exchange between berthierine and injected fluid (Figure 10a), the amounts of H- and O-isotope exchange were probably of similar magnitude. This observation suggests that exchange occurred by hydroxyl (OH^-) replacement, as expected at >100ºC (Longstaffe and Ayalon, 1990).

Smectitic clays. In near-injector cores, smectitic clays generally have lower $\delta^{18}O$ values than they do in pre-steam and distal-injector cores (Figure 10b). The exceptions to this observation provide further information about the penetration of injected fluids into the reservoir. Near-injector samples from >9 m below the upper injection zone in core G-OB3 (samples 30 and 32) have $\delta^{18}O$ values similar to pre-steam smectitic clays (Figure 10b). This indicates very limited, if any, interaction with the injected fluid, which is consistent with siderite preservation in this portion of the reservoir. Lower vertical permeability due to abundant detrital clays and shale layers, as well as limited bitumen mobilization, probably restricted fluid penetration below the upper injection zone.

Only one distal-injector smectitic sample (shale sample D26-6A-513m; Figure 10b), from a depth corresponding to the lower injection zone, experienced O-isotope exchange. Berthierine was similarly affected at the depth of the upper injection zone (sample D23-6A-19; Figure 10a). Hot fluids appear to have penetrated greater horizontal distances in both injection zones in core D23-6A while in post-steam core G-OB3 fluid movement into the formation occurred primarily at the upper injection zone. These differences relate to how CSS was conducted. In the case of core D23-6A, steam was first injected at the lower zone for two cycles and

https://doi.org/10.1346/CCMN.2013.0610504 Published online by Cambridge University Press

then a second injection zone was created higher up, followed by four more CSS cycles. Thus, isotopic evidence exists for fluid penetration at both depths. In the case of core G-OB3, all three injection zones were created at the same time and the isotopic data clearly show that fluids entered the formation preferentially *via* the uppermost injection zone.

If the smectitic clays neoformed from, or exchanged completely with, the injected fluid ($\delta^{18}O = -12‰$) then their equilibrium $\delta^{18}O$ values should range from ~−7‰ (250°C) to +2‰ (100°C) (calculated using $1000\ln\alpha_{smectite-H_2O} = 2.58(10^6)T^{-2} - 4.19$; Savin and Lee, 1988). The near-injector post-steam smectitic clays, except for one shale, have higher $\delta^{18}O$ values. In particular, the values for samples rich in HIS range from +7.5 to +16.1‰. Such compositions suggest that: (1) HIS formed by addition of hydroxy-interlayer material to pre-existing smectitic clays and inherited most of its oxygen from these precursors; or (2) HIS formation occurred during the earliest stage of CSS when reservoir temperatures were relatively low (well below 100ºC). The fact that HIS is observed in distal-injector cores that lack other evidence of CSS (Table 2) supports both of these assertions. Addition of hydroxy-interlayer material to pre-steam, diagenetic smectitic clays may also have attenuated O-isotope exchange during later stages of CSS by restricting fluid access to the clay interlayer.

The H-isotope geochemistry of smectitic clays is even less well understood than that of oxygen. The smectitic clay-water H-isotope fractionation is more sensitive to chemical composition (particularly octahedral cation composition) than temperature, ranging from −30 ± 5‰ for Fe-poor smectite to −90 ± 10‰ for Fe-rich clays such as nontronite (Suzuoki and Epstein, 1976; Kyser, 1987; Marumo *et al.*, 1980, 1995; Gilg and Sheppard, 1996; Sheppard and Gilg, 1996). Nevertheless, H-isotope exchange between smectitic clays and water should occur more rapidly and at lower temperatures than O-exchange (O'Neil and Kharaka, 1976). Thus, the lack of a systematic decrease in the δ^2H values of near-injector post-steam smectitic clays, as was observed for berthierine, was unexpected. However, interpretation of the data is complicated because the samples are mixtures of naturally occurring detrital and diagenetic clays with variable starting δ^2H values that have been modified to differing degrees by CSS. The problem is simplified by focusing on a single near-injector core. In near-injector core G-OB3 the expected shift to lower δ^2H values was observed, but only above the upper injection zone and only in samples containing HIS (samples 6, 10, and 15; Figure 10b). Samples from just below the depth of the upper injection zone (G-OB3-23 and -26), which do not contain HIS, have δ^2H values similar to samples from well below the depth of steam injection (G-OB-30 and -32) that presumably were unaffected by exchange (Figure 10b). Even more interesting is the fact that samples G-OB3-23 and -26 exhibit evidence of O-isotope exchange, despite the apparent lack of H-isotope exchange. Shale samples, which consist only of detrital smectite and/or illite-smectite, also show no evidence of H-isotope exchange, despite significant O-isotope exchange. This result is counter-intuitive given that H-exchange between clays and water typically occurs more rapidly and at lower temperatures than O-exchange.

Complete H-isotope exchange between the injected fluid ($\delta^2H = -107‰$) at 100−150ºC and smectitic clays − the hydrogen isotopic fractionation of which is assumed to be like that of illite-smectite − would produce smectitic clays with δ^2H values ranging from −134 to −119‰ ($1000\ln\alpha_{illite/smectite-H_2O} = -45.3[10^3]T^{-1} + 94.7$; Capuano, 1992); such compositions are similar to pre-steam values (−123 to −98‰). This could explain why pre- and post-steam shale samples, which did not change mineralogically, have very similar δ^2H values.

SUMMARY

Cyclic steam stimulation of Clearwater Formation oil sands produced substantial mineralogical changes in near-injector cores, including dissolution of volcanic glass and disseminated carbonates, as well as neoformation of zeolites, pore-lining calcite, and HIS. Berthierine, the dominant clay mineral in pre-steam oil sands, was preserved during CSS and remains the most abundant clay mineral in the post-steam oil sands even in core May B-12A, which was sampled after 18 steam cycles. However, the $\delta^{18}O$ and δ^2H values of berthierine from near-injector cores decreased during CSS as the result of partial isotopic exchange with the injected fluid at >100ºC. The $\delta^{18}O$ values of smectitic clays in near-injector cores also decreased because of isotopic exchange or formation of HIS. However, a systematic change in δ^2H values of near-injector smectitic clays was not observed. Only above the uppermost injection zone in near-injector core G-OB3 was a decrease in δ^2H detectable. The highly variable H isotopic composition of pre-steam smectitic clays appears to have obscured H-isotope exchange. In addition, the particular combination of fluid composition and temperature during CSS has probably yielded post-steam δ^2H values similar to pre-steam values, thus explaining the lack of a δ^2H shift for the shales.

In distal-injector cores berthierine and smectitic clays were generally unaffected by H- or O-isotope exchange during CSS, which probably reflects the inability of the injected fluid to penetrate tens of meters into the formation because bitumen saturation was still too high. Distal-injector core D23-6A provides an exception to this general observation, as O- and H-isotope exchange are detected at a depth coincident with the injection zone. This result suggests that injected fluids

https://doi.org/10.1346/CCMN.2013.0610504 Published online by Cambridge University Press

were able to move horizontally further into the reservoir within the injection zone, probably along fractures generated during the injection process. Whether or not H-isotope exchange between the clay minerals and bitumen occurred in portions of the reservoir that were heated, but which had no contact with injected fluid (*i.e.* distal-injector cores and below the depth of steam injection in near-injector cores), is difficult to assess. If it did occur, it did not noticeably affect the δ^2H values of the clays.

Cyclic steam stimulation resulted in the formation of HIS in many of the near-injector cores and, less commonly, in distal-injector cores. The O-isotope data suggest that this clay formed by the addition of interlayer material to pre-existing smectitic clays during the early stages of CSS when reservoir temperatures were still relatively low ($\leqslant$100ºC). This may explain why HIS is less abundant in portions of the reservoir that are berthierine-rich (*e.g.* post-steam core BB-13A); however, it is also possible that grain-coating berthierine isolated reactive rock fragments from the hot injected fluid and, thus, restricted HIS formation.

ACKNOWLEDGMENTS

The authors are grateful to Drs. Savin, Wampler, and Stucki, and two anonymous reviewers whose comments and suggestions have greatly improved this manuscript. Funding was provided by the Alberta Oil Sands Technology and Research Authority (AOSTRA/University/Industry Agreement #1103) and the Natural Sciences and Engineering Research Council of Canada. The authors are also grateful for logistical and technical support from Imperial Resources Canada and (then) Amoco Canada, in particular, J. Dudley, A. Fox, A. Cochran, D. Layton, S. Howell, and J. Bodeux. Analytical support at the University of Western Ontario was provided by P. Middlestead, R. Fagan, Y. Thibault, and S. Forbes. Preparation of this paper was supported in part by funding from the Canada Research Chairs program. This is 'Laboratory for Stable Isotope Science' Contribution #288.

REFERENCES

Abercrombie, H.J., Shevalier, M., and Hutcheon, I.E. (1989) Natural diagenesis: A model for artificial diagenesis during steam-assisted recovery of heavy oil, Cold Lake, Alberta, Canada. Pp. 1–4 in: *Proceedings of the 6th International Symposium on Water–Rock Interaction* (D.L. Miles, editor). Balkema, Rotterdam.

Beckie, K.N. and McIntosh, R.A. (1989) Geology and resources of the Primrose crude bitumen deposits, northeastern Alberta. Pp. 19–36 in: *Fourth UNITAR/UNDP Conference on Heavy Crude and Tar Sands, Vol. 2 Geology, chemistry* (R.F. Meyer and E.J. Wiggins, editors). Alberta Oil Sands Technology and Research Authority.

Bird, M.I. and Chivas, A.R. (1988) Stable-isotope evidence for low-temperature kaolinitic weathering and post-formational hydrogen-isotope exchange in Permian kaolinites. *Chemical Geology (Isotope Geoscience Section)*, **72**, 249–265.

Biscaye, P.E. (1965) Mineralogy and sedimentation of recent deep-sea clay in the Atlantic Ocean and adjacent seas and oceans. *Geological Society of America Bulletin*, **76**, 803–832.

Boon, J.A. (1977) Fluid-rock interactions during steam injection. Pp. 133–138 in: *The Oil Sands of Canada/Venezuela* (D.A. Redford and A.G. Winestock, editors). Special Volume **17**, Canadian Institute of Mining and Metallurgy.

Boon, J.A. and Hitchon, B. (1983) Application of fluid-rock reaction studies to in situ recovery from oil sand deposits, Alberta, Canada – II. Mineral transformations during an experimental-statistical study of water-bitumen-shale reactions. *Geochimica et Cosmochimica Acta*, **47**, 249–257.

Boon, J.A., Hamilton, T. Holloway, L., and Wiwchar, B. (1983) Reaction between rock matrix and injected fluids in Cold Lake oil sands – potential for formation damage. *Journal of Canadian Petroleum Technology*, **22**, 55–66.

Capuano, R.M. (1992) The temperature dependence of hydrogen isotope fractionation between clay minerals and water: Evidence from a geopressured system. *Geochimica et Cosmochimica Acta*, **56**, 2547–2554.

Cathles, L.M., Schoell, M., and Simon, R. (1990) A kinetic model of CO_2 generation and mineral and isotopic alteration during steamflooding. *SPE Reservoir Engineering*, **5**, 524–530.

Chakrabarty, T. and Longo, J.M. (1994) Production problems in the steam-stimulated shaley oil sands of the Cold Lake reservoir: Cause and possible solutions. *The Journal of Canadian Petroleum Technology*, **33**, 34–39.

Clayton, R.N. and Mayeda, T.K. (1963) The use of bromine pentafluoride in the extraction of oxygen from oxides and silicates for isotopic analysis. *Geochimica et Cosmochimica Acta*, **27**, 43–52.

Coleman, M.L., Shepherd, T.J., Durham, J.J., Rouse, J.E., and Moore, G.R. (1982) Reduction of water with zinc for hydrogen isotope analysis. *Analytical Chemistry*, **54**, 993–995.

Draper, R.G., Yates, A., and Chantler, H.McD. (1955) A comparison of three laboratory methods for determining the bitumen content of bituminous sands. Canada. Department of Mines and Technical Surveys, Mines Branch, Report No. FRL-211 of the Fuels Division.

Dudley, J.S. and Moore, C.H. (1992) Computer modeling of steam flood experiments. Pp. 1223–1226 in: *Proceedings of the 7th International Symposium on Water–Rock Interaction* (Y.K. Kharaka and A.S. Maest, editors). Balkema, Rotterdam.

ECRB (2012) Alberta Energy Reserves 2011 and Supply/Demand Outlook for 2012–21. Energy Resources Conservation Board Reserve Report ST98–2012, Calgary, Alberta.

Fagan, R. (2001) Oxygen- and hydrogen-isotope study of hydroxyl group behavior in standard smectite and kaolinite. PhD Thesis, The University of Western Ontario, Canada, 215 pp.

Fagan, R. and Longstaffe, F.J. (1996) The effects of laboratory pretreatments on the hydrogen- and oxygen-isotope compositions of clay minerals. Pp. 55 in: *Clays in and for the Environment.* 33rd Annual Meeting of the Clay Minerals Society, Program and Abstracts.

Fialka, B.N., McClanahan, R.K., Robb, G.A., and Longstaffe, F.J. (1993) The evaluation of cyclic steam stimulation in an oil sand reservoir using post-steam core analysis. *Canadian Journal of Petroleum Technology*, **32**, 56–62.

Gallant, R.J., Stark, S.D., and Taylor, M.D. (1993) Steaming and operation strategies at a midlife CSS Operation. Society of Petroleum Engineers International Thermal Operations Symposium, Paper 25794.

Gilg, H.A. and Sheppard, S.M.F. (1996) Hydrogen isotope fractionation between kaolinite and water revisited. *Geochimica et Cosmochimica Acta*, **60**, 529–533.

Godfrey, J.D. (1962) The deuterium content of hydrous

minerals from the east-central Sierra Nevada and Yosemite National Park. *Geochimica et Cosmochimica Acta*, **26**, 1215–1245.

Gunter, W.D. and Bird, G.W. (1988) CO_2 production in tar sand reservoirs under in situ steam temperatures: reactive calcite dissolution. *Chemical Geology*, **70**, 301–311.

Gunter, W.D., Bird, G.W., Aggarwal, P.K., and Leone, J.A. (1989) Modeling of smectite synthesis in reservoir sands: comparison of PATH predictions to autoclave experiments. Pp. 383–398 in: *Fourth UNITAR/UNDP International Conference on Heavy Crudes and Tar Sands, Vol. 3 Mining, drilling* (R.F. Meyer and E.J. Wiggins, editors). Alberta Oil Sands Technology and Research Authority.

Harrison, D.B., Glaister, R.P., and Nelson, H.W. (1981) Reservoir description of the Clearwater oil sands, Cold Lake, Alberta, Canada. Pp. 264–279 in: *The Future of Heavy Crude and Tar Sands* (R.F. Meyer, C.T. Steel, and J.C. Olson, editors). McGraw Hill, New York.

He, S. (2001) Water–rock interactions during steaming of Clearwater oil sands. PhD thesis, The University of Western Ontario, London, Ontario, Canada, 259 pp.

Hebner, B.A., Bird, G.W., and Longstaffe, F.J. (1986) Fluid/pore-mineral transformations during simulated steam injection: Implications for reduced permeability damage. *Journal of Canadian Petroleum Technology*, **25**, 1–6.

Horita, J., Cole, D.R., and Wesolowski, D.J. (1995) The activity-composition relationship of oxygen and hydrogen isotopes in aqueous salt solutions: III. Vapor-water equilibration of NaCl solutions to 350ºC. *Geochimica et Cosmochimica Acta*, **59**, 1139–1151.

Horita, J., Driesner, T., and Cole, D.R. (1999) Pressure effect on hydrogen isotope fractionation between brucite and water at elevated temperatures. *Science*, **286**, 1545–1547.

Horita, J., Cole, D.R., Polyakov, V.B., and Driesner, T. (2002) Experimental and theoretical study of pressure effects on hydrogen isotope fractionation in the system brucite-water at elevated temperatures. *Geochimica et Cosmochimica Acta*, **66**, 3769–3788.

Hornibrook, E.R.C. and Longstaffe, F.J. (1996) Berthierine from the Lower Cretaceous Clearwater Formation, Alberta, Canada. *Clays and Clay Minerals*, **44**, 1–21.

Huang, W. and Longo, J.M. (1994) Experimental studies of silicate-carbonate reactions – II. Applications to steam flooding of oil sands. *Applied Geochemistry*, **9**, 523–532.

Hutcheon, I. (1984) A review of artificial diagenesis during thermally enhanced recovery. Pp. 413–429 in: *Clastic Diagenesis* (D.A. McDonald and R.C. Surdam, editors). American Association of Petroleum Geologists Memoir **37**, Tulsa, Oklahoma, USA.

Hutcheon, I. and Abercrombie, H.J. (1990) Fluid-rock interaction in thermal recovery of bitumen, Tucker Lake Pilot, Cold Lake, Alberta. Pp. 161–170 in: *Prediction of Reservoir Quality Through Chemical Modeling* (I.D. Meshri and P.J. Ortoleva, editors). American Association of Petroleum Geologists Memoir 49, Tulsa, Oklahoma, USA.

Hutcheon, I., Abercrombie, H.J., Shevalier, M., and Nahnybida, C. (1989) A comparison of formation reactivity in quartz-rich and quartz-poor reservoirs during steam assisted recovery. Pp. 747–757 in: *Fourth UNITAR/UNDP International Conference on Heavy Crude and Tar Sands.* Vol. 4 *In situ Recovery* (R.F. Meyer and E.J. Wiggins, editors). Alberta Oil Sands Technology and Research Authority.

Hutcheon, I., Abercrombie, H.J., and Krouse, H.R. (1990) Inorganic origin of carbon dioxide during low temperature thermal recovery of bitumen: Chemical and isotopic evidence. *Geochimica et Cosmochimica Acta*, **54**, 165–171.

Jiang, Q., Thornton, B., Russel-Houston, J., and Spence, S. (2010) Review of thermal recovery technologies for the Clearwater and Lower Grand Rapids formations in Cold Lake, Alberta. *Journal of Canadian Petroleum Technology*, **49**, 57–68.

Kirk, J.S., Bird, G.W., and Longstaffe, F.J. (1987) Laboratory study of the effects of steam condensate flooding in the Clearwater Formation: High temperature flow experiments. *Bulletin of Canadian Petroleum Geology*, **35**, 34–47.

Kry, P.R. (1992) In-situ recovery technology at Cold Lake, Alberta, Canada. All Union Petroleum-Research Geological Exploration Institute (VNIGRI) Conference on Unconventional Hydrocarbon Accumulations, St. Petersburg.

Kyser, T.K. (1987) Equilibrium fractionation factors for stable isotopes. Pp. 1–84 in: *Mineralogical Association of Canada Short Course in Stable Isotope Geochemistry*, vol. **13** (T.K. Kyser, editor). Mineralogical Association of Canada, Ottawa, Ontario, Canada.

Kyser, T.K. and Kerrich, R. (1991) Retrograde exchange of hydrogen isotopes between hydrous minerals and water at low temperatures. Pp. 409–422 in: *Stable Isotope Geochemistry: A tribute to Samuel Epstein* (H.P. Taylor Jr., J.R. O'Neil, and I.R. Kaplan). Special Publication **3**, The Geochemical Society, St. Louis, Missouri, USA.

Kyser, T.K. and O'Neil, J.R. (1984) Hydrogen isotope systematics of submarine basalts. *Geochimica et Cosmochimica Acta*, **48**, 2123–2133.

Lefebvre, R. and Hutcheon, I. (1986) Mineral reactions in quartzose rocks during thermal recovery of heavy oil, Lloydminster, Saskatchewan, Canada. *Applied Geochemistry*, **1**, 395–405.

Longstaffe, F.J. (1994) Stable isotopic constraints on sandstone diagenesis in the western Canada sedimentary basin. Pp. 223–274 in: *Quantitative Diagenesis: Recent Developments and Applications to Reservoir Geology* (A. Parker and B.W. Sellwood, editors). Kluwer Academic Publishers, NATO Advanced Study Institute Series.

Longstaffe, F.J. and Ayalon, A. (1990) Hydrogen-isotope geochemistry of diagenetic clay minerals from Cretaceous sandstones, Alberta, Canada: evidence for exchange. *Applied Geochemistry*, **5**, 657–668.

Longstaffe, F.J., Racki, M.A., Ayalon, A., Wickert, L.M., Wightman, D.M., and Bird, G.W. (1990) Water-mineral-organic matter interactions during clastic diagenesis of Cretaceous heavy oil reservoirs, Cold Lake area, Alberta. *American Association of Petroleum Geologists Bulletin*, **74**, 1306–1307 [abstract].

Longstaffe, F.J., Ayalon, A., and Racki, M.A. (1992) Stable isotope studies of diagenesis in berthierine-bearing oil sands, Clearwater Formation, Alberta. Pp. 955–958 in: *Proceedings of the 7th International Symposium on Water–Rock Interaction* (Y.K. Kharaka and A.S. Maest, editors). Balkema, Rotterdam.

Marcano, N. (2011) Isotopic and molecular studies of biodegraded oils and the development of chemical proxies for monitoring *in situ* upgrading of bitumen. PhD Thesis, The University Calgary, Calgary, Alberta, Canada, 368 pp.

Marumo, K., Nagasawa, K., and Kuroda, Y. (1980) Mineralogy and hydrogen isotope geochemistry of clay minerals in the Ohnuma geothermal area, northeastern Japan. *Earth and Planetary Science Letters*, **47**, 255–262.

Marumo, K., Longstaffe, F.J., and Matsubaya, O. (1995) Stable isotope geochemistry of clay minerals from fossil and active hydrothermal systems, southwestern Hokkaido, Japan. *Geochimica et Cosmochimica Acta*, **59**, 2545–2559.

McCrimmon, G.G. and Arnott, R.W.C. (1995) The Clearwater Formation, Cold Lake, Alberta: a world class hydrocarbon reservoir hosted in a complex succession of tide-dominated deltaic deposits. *Bulletin of Canadian Petroleum Geology*, **50**, 370–392.

McKay, J.L. and Longstaffe F.J. (1997) Diagenesis of the Lower Cretaceous Clearwater Formation, Primrose area, northeastern Alberta. Pp. 392–412 in: *The Mannville* (S.G. Pemberton and D.P. James, editors). Memoir **18**, Canadian Society of Petroleum Geologists, Calgary, Alberta, Canada.

Mizota, C. and Longstaffe, F.J. (1996) Origin of Cretaceous and Oligocene kaolinites from the Iwaizumi clay deposit, Iwate, northeastern Japan. *Clays and Clay Minerals*, **44**, 408–416.

Mok, U., Wiwchar, B., Gunter, W.D., and Longstaffe, F.J. (1995) The distribution, morphology, and composition of minerals formed by hydrothermal alteration of an immature sand during a flow-through experiment. Geological Association of Canada-Mineralogical Association of Canada, Program with Abstracts, v. **20**, p. A72.

O'Neil, J.R. (1987) Preservation of H, C, and O isotopic ratios in the low temperature environment. Pp. 85–128 in: *Mineralogical Association of Canada Short Course in Stable Isotope Geochemistry*, vol. **13** (T.K. Kyser, editor).

O'Neil, J.R. and Kharaka, Y.K. (1976) Hydrogen and oxygen isotope exchange reactions between clay minerals and water. *Geochimica et Cosmochimica Acta*, **40**, 241–246.

Perry, C. and Gillott, J.E. (1979) The formation and behaviour of montmorillonite during the use of wet forward combustion in the Alberta oil sand deposits. *Bulletin of Canadian Petroleum Geology*, **27**, 314–325.

Prentice, M.E. and Wightman, D.M. (1987) Mineralogy of the Clearwater Formation, Cold Lake oil sands area: implications for enhanced oil recovery. Alberta Geological Survey, Report, 41 pp.

Putnam, P.E. and Pedskalny, M.A. (1983) Provenance of Clearwater Formation reservoir sandstones, Cold Lake, Alberta, with comments on feldspar composition. *Bulletin of Canadian Petroleum Geology*, **5**, 148–160.

Racki, M. (1991) Diagenesis of the Clearwater Formation, Cold Lake, Alberta. M.Sc. Thesis, Dept. of Geology, The University of Western Ontario, London, Ontario, Canada.

Roether, W. (1970) Water-CO_2 exchange set-up for the routine O-18 assay of natural waters. *International Journal of Applied Radiation and Isotopes*, **21**, 379–387.

Savin, S.M. and Epstein, S. (1970) The oxygen and hydrogen isotope geochemistry of clay minerals. *Geochimica et Cosmochimica Acta*, **34**, 25–42.

Savin, S.M. and Hsieh, J.C.C. (1998) The hydrogen and oxygen isotope geochemistry of pedogenic clay minerals: principles and theoretical background. *Geoderma*, **82**, 227–253.

Savin, S.M. and Lee, M. (1988) Isotope studies of phyllosilicates. Pp. 189–223 in: *Hydrous Phyllosilicates* (*Exclusive of Micas*) (S.W. Bailey, editor). Reviews in Mineralogy, **19**, Mineralogical Society of America, Washington, D.C.

Sedimentology Research Group (1981) The effects of *in situ* steam injection on Cold Lake oil sands. *Bulletin of Canadian Petroleum Geology*, **29**, 447–478.

Shepherd, D.W. (1981) Steam stimulation recovery of Cold Lake bitumen. Pp. 349–360 in: *The Future of Heavy Crude and Tar Sands* (R.F. Meyer, J.C. Wynn, and J.C. Olson, editors). MaGraw-Hill, New York.

Sheppard, S.M.F. and Gilg, H.A. (1996) Stable isotope geochemistry of clay minerals. *Clay Minerals*, **31**, 1–24.

Shevalier, M., Hutcheon, I., Nahnybida, C., and Abercrombie, H. (1992) Contrasts between steam stimulation and in-situ combustion process: an analysis of co-produced fluid compositional data. Pp. 1125–1128 in: *Proceedings of the Seventh International Symposium on Water–Rock Interaction* (Y.K. Kharaka and A.S. Maest, editors). Balkema, Rotterdam.

Suzuoki, T. and Epstein, S. (1976) Hydrogen isotope fractionation between OH-bearing minerals and water. *Geochimica et Cosmochimica Acta*, **40**, 1229–1240.

Tilley, B.J. and Gunter, W.D. (1988) Mineralogy and water chemistry of the burnt zone from a wet combustion pilot in Alberta. *Bulletin of Canadian Petroleum Geology*, **36**, 25–39.

Visser, K., Dankers, P.H.M., Leckie, D., and VanDer Marel, A.G.P. (1985) Mineralogy and geology of the Clearwater reservoir sands in the Wolf Lake Area, Cold Lake, Alberta. Pp. 118–133 in: *Third UNITAR/UNDP International Conference on Heavy Crude and Tar Sands* (R.F. Meyer, editors). Alberta Oil Sands Technology and Research Authority.

Vittoratos, E. (1986) Interpretation of temperature profiles from the steam-stimulated Cold Lake reservoir. Pp. 243–254 in: *Proceedings 56th California Regional Meeting of the Society of Petroleum Engineers*, Paper 15050.

Wickert, L.M. (1992) Stratigraphy and diagenesis of the Clearwater Formation. MSc Thesis, Department of Geology, University of Alberta, Edmonton, Alberta, Canada, 365 pp.

Yeh, H.-W. and Savin, S.M. (1977) Mechanism of burial metamorphism of argillaceous sediments: 3. O-isotope evidence. *Bulletin of the Geological Society of America*, **88**, 1321–1330.

Zhou, Z., Gunter, W.D., Kadatz, B., and Cameron, S. (1995) Hydrothermal stability of the clay minerals from the Clearwater reservoirs at Cold Lake, Alberta. Pp. 27–35 in: *Heavy Crude and Tar Sands – Fueling for a Clean and Safe Environment, volume 2* (R.F. Meyer, editor). 6th UNITAR International Conference on Heavy Crude and Tar Sands.

Zhou, Z., Dudley, J.S., Wiwchar, B., and Gunter, W.D. (1999) The potential of permeability damage during thermal recovery of Cold Lake bitumen. *Journal of Canadian Petroleum Technology*, **38**, 55–60.

(*Received 28 December 2012; revised 15 August 2013; Ms. 738; AE: J.M. Wampler*)